Pharmacological induction of hypoxia-inducible transcription factor ARNT attenuates chronic kidney failure

Supplemental data

Björn Tampe[1,#], Désirée Tampe[1,#], Gunsmaa Nyamsuren[1], Friederike Klöpper[1], Gregor Rapp[1], Anne Kauffels[2], Thomas Lorf[2], Elisabeth M. Zeisberg[3,4], Gerhard A. Müller[1], Raghu Kalluri[5], Samy Hakroush[6], Michael Zeisberg[1,4]

[1]*Department of Nephrology and Rheumatology, University Medical Center Göttingen, Georg August University, Göttingen, Germany*

[2]*Department of General, Visceral and Pediatric Surgery, University Medical Center Göttingen, Georg August University, Göttingen, Germany*

[3]*Department of Cardiology and Pneumology, University Medical Center Göttingen, Georg August University, Göttingen, Germany*

[4]*German Center for Cardiovascular Research (DZHK), Robert Koch Street 40, Göttingen, Germany*

[5]*Department of Cancer Biology and the Metastasis Research Center, University of Texas MD Anderson Cancer Center, Houston, USA*

[6]*Institute of Pathology, University Medical Center Göttingen, Georg August University, Göttingen, Germany*

[#]equal contribution

Running title: ARNT attenuates organ failure

Corresponding author:

Michael Zeisberg, MD
Clinic for Nephrology and Rheumatology
University Medicine Göttingen
Georg August University
Göttingen, Germany
Email: mzeisberg@med.uni-goettingen.de

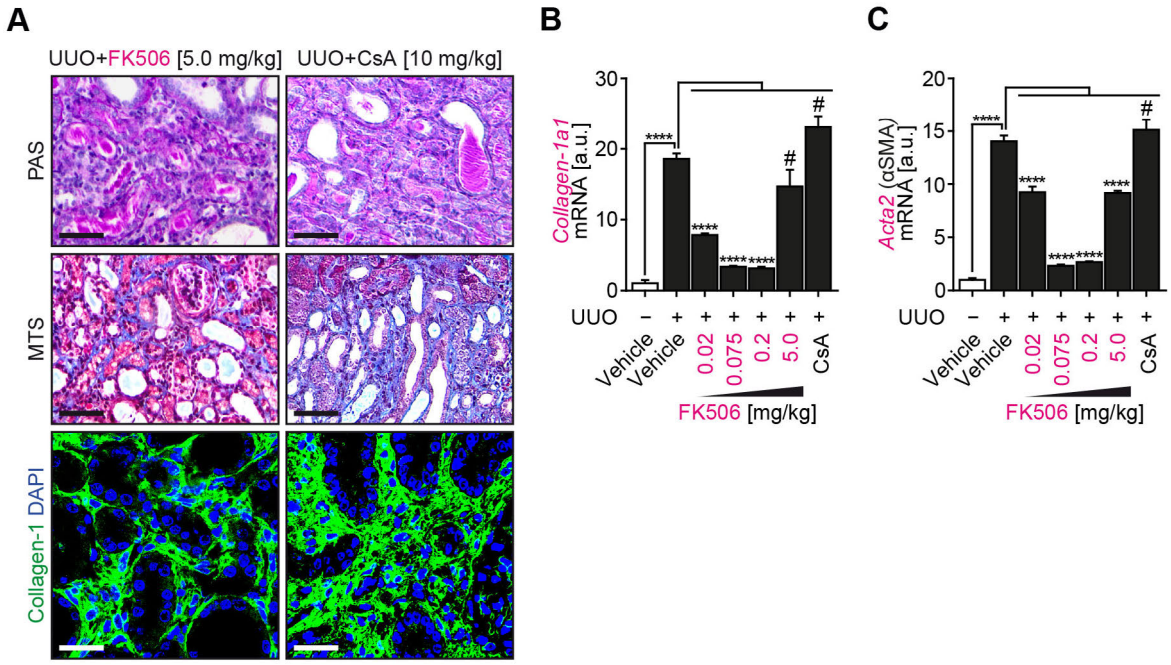

Supplementary Figure 1. (**A**) Representative photomicrographs of PAS (scale bars 50 µm), MTS (scale bars 50 µm) stainings and sections immunolabelled with primary antibodies against Collagen-1 (scale bars 25 µm) from mice challenged with UUO 10 days after ureteral obstruction and treated with FK506 (5.0 mg/kg orally per day) or equimolar CsA (10 mg/kg orally per day). (**B,C**) Intrarenal expression levels of *Collagen-1a1* or *Acta2* (encoding αSMA) were analyzed by qRT-PCR in total kidney lysates (n=3-4/group, data are presented as means±s.d., **** *p<0.0001*, # *no significance*, values of *p* were calculated using one-way ANOVA with Bonferroni post-hoc analysis).

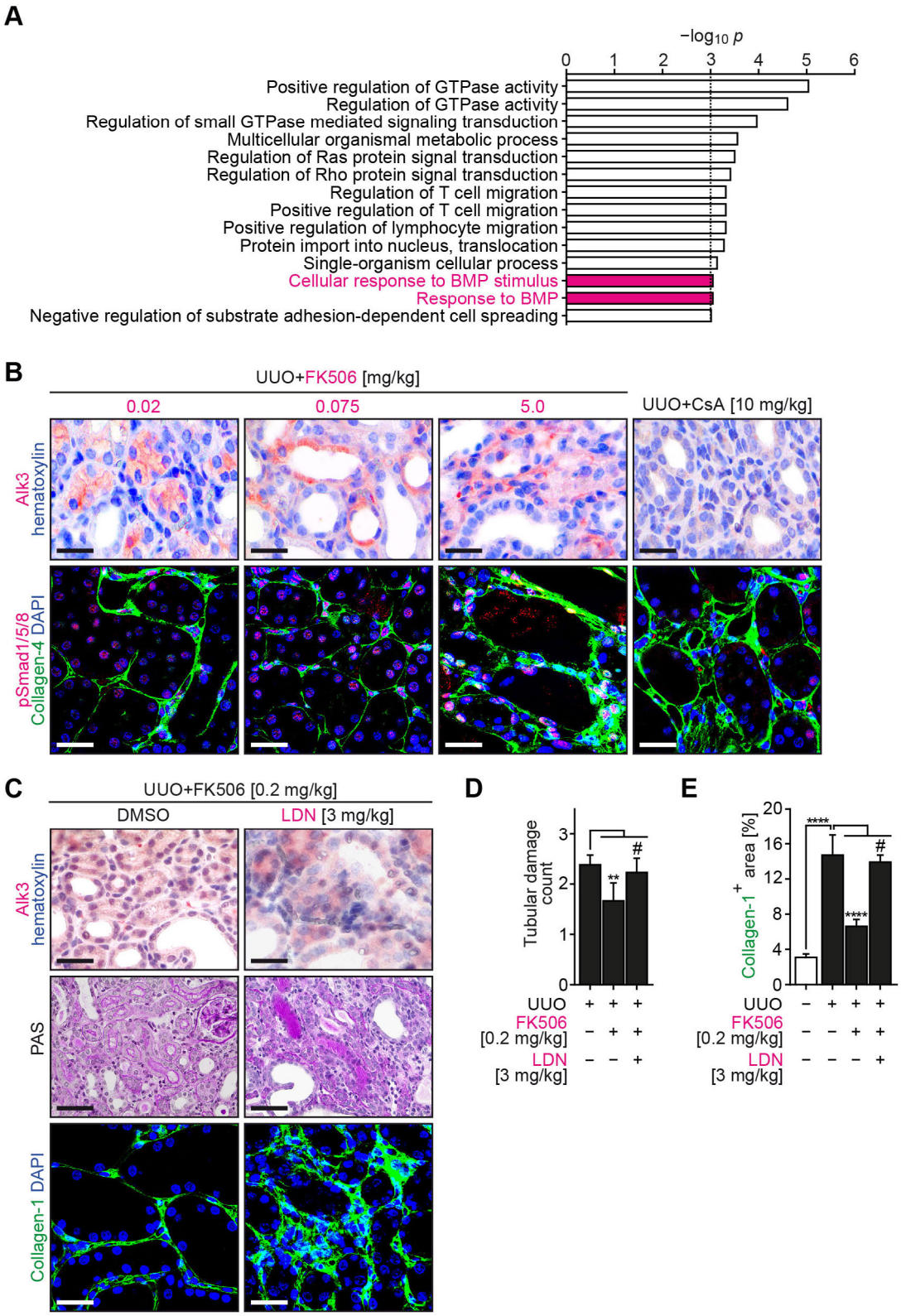

Supplementary Figure 2. (**A**) Based on genome-wide transcriptional expression datasets for bioactive small molecules (accession number GSE5258), pathway analysis of differentially expressed genes induced in response to FK506 is shown (data are presented as process analyses of -$\log_{10}$ *p*). (**B**) Representative photomicrographs of fibrotic kidney sections from mice challenged with UUO 10 days after ureteral obstruction and treated with FK506 (0.02, 0.075, 5.0 mg/kg orally per day, respectively) or equimolar CsA (10 mg/kg orally per day) and immunolabelled with primary antibodies against Alk3 (scale bars 25 µm) and pSmad1/5/8 (scale bars 25 µm). (**C-E**) Mice were challenged with UUO and treated with either vehicle buffer or FK506 (0.2 mg/kg orally per day) when ALK3 signaling transduction was pharmacologically blocked with small molecule LDN-193189 (LDN, 3 mg/kg intraperitoneally per day). The panels show representative photomicrographs of sections immunolabelled with primary antibodies against Alk3 (scale bars 25 µm), PAS (scale bars 50 µm) and Collagen-1 (scale bars 25 µm, n=6/group, data are presented as means±s.d., ** *p<0.01*, **** *p<0.0001*, # *no significance*, values of *p* were calculated using one-way ANOVA with Bonferroni post-hoc analysis).

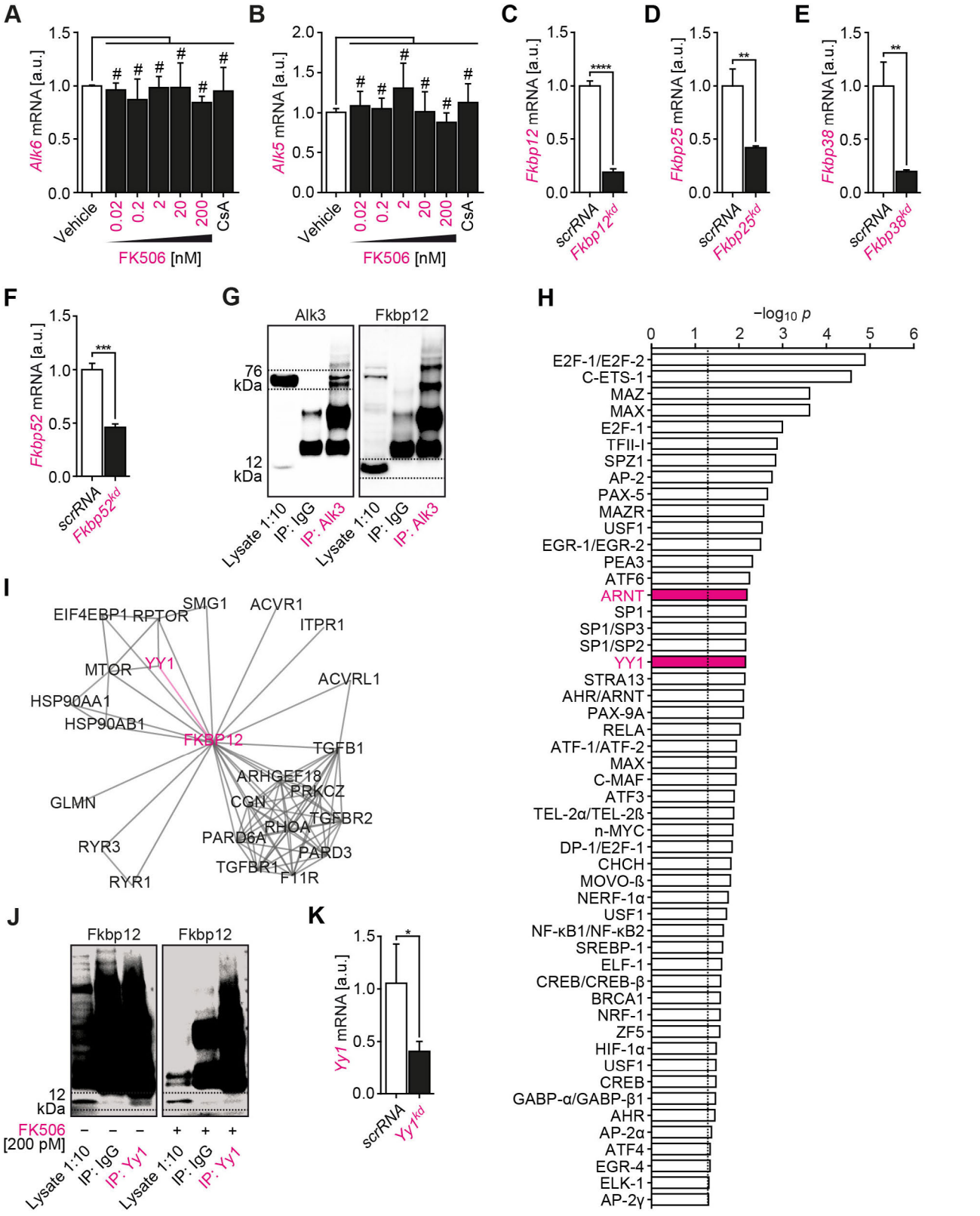

Supplementary Figure 3. (**A,B**) TECs were exposed to either vehicle, indicated concentrations of FK506 (0.02, 0.2, 2, 20, 200 nM, respectively) or equimolar Cyclosporine A (CsA, 10 nM), mRNA expression levels of type I BMP receptors *Alk6* and *Alk5* were analyzed by qRT-PCR (n=3 independent experiments, data are presented as means±s.d., # *no significance*, values of *p* were calculated using one-way ANOVA with Bonferroni post-hoc analysis). (**C-F**) TECs were transfected with either scrambled RNA (*scrRNA*), siRNA targeting Fkbp12 (*Fkbp12*^{kd}), Fkbp25 (*Fkbp25*^{kd}), Fkbp38 (*Fkbp38*^{kd}), Fkbp52 (*Fkbp52*^{kd}), the bar graphs summarize relative mRNA expression levels of respective transcripts (n=3 independent experiments, data are presented as means±s.d., ** *p<0.01*, *** *p<0.001*, **** *p<0.0001*, values of *p* were calculated using Student's t test). (**G**) As analyzed by co-immunoprecipitation after Alk3 pull-down (IP: Alk3), direct interaction between Fkbp12 and Alk3 was assessed. (**H**) Based on genome-wide transcriptional expression datasets for bioactive small molecules (accession number GSE5258), motif enrichment analysis of differentially expressed genes induced in response to FK506 is shown (data are presented as process analyses of -log$_{10}$ *p*). (**I**) Network between FKBP12 and identified interacting proteins, including YY1. (**J**) As analyzed by co-immunoprecipitation after Yy1 pull-down (IP: Yy1), direct interaction between Yy1 and Fkbp12 was assessed. (**K**) Analyzed by qRT-PCR, the bar graphs summarize relative *Yy1* mRNA expression levels (n=3 independent experiments, data are presented as means±s.d., * *p<0.05*, values of *p* were calculated using Student's t test).

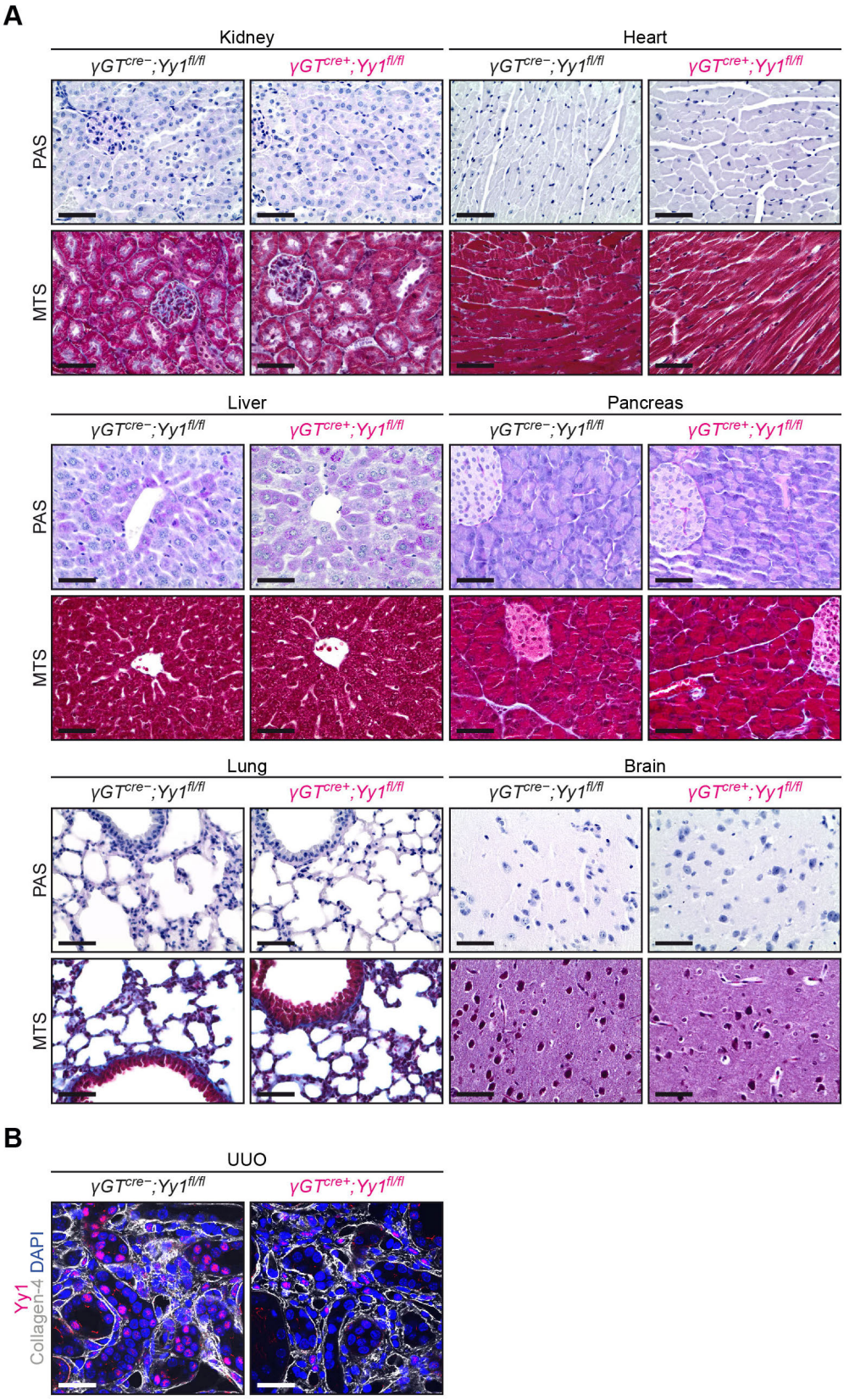

Supplementary Figure 4. (**A**) Representative photomicrographs of kidney, heart, liver, pancreas, lung and brain sections labelled for PAS (scale bars: 50 µm) and MTS (scale bars: 50 µm) of mice conditionally depleted for *YY1* in TECs ($\gamma GT^{cre+};Yy1^{fl/fl}$) and corresponding littermate controls ($\gamma GT^{cre-};Yy1^{fl/fl}$) are shown. (**B**) Representative photomicrographs of kidneys challenged with UUO and immunolabelled with primary antibodies against Yy1 (scale bars 25 µm) are shown.

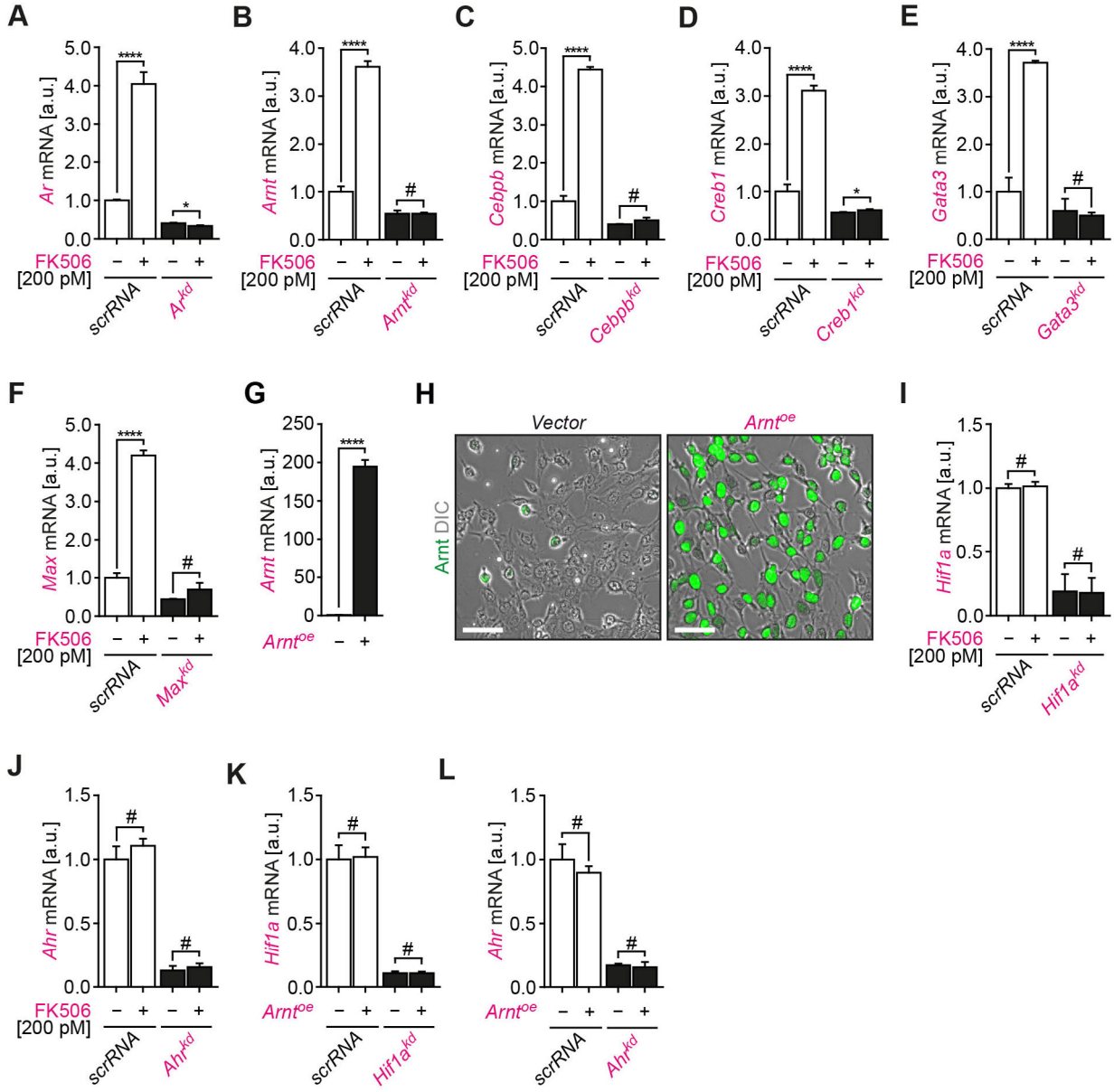

Supplementary Figure 5. (**A-F**) TECs were transfected with either scrambled RNA (*scrRNA*), siRNA targeting Ar (Ar^{kd}), Arnt ($Arnt^{kd}$), Cebpb ($Cebpb^{kd}$), Creb1 ($Creb1^{kd}$), Gata3 ($Gata3^{kd}$) or Max (Max^{kd}). Analyzed by qRT-PCR, the bar graphs summarize relative mRNA expression levels of respective transcripts in response to FK506 (200 pM, n=3 independent experiments, data are presented as means±s.d., * *p<0.05*, **** *p<0.0001*, # *no significance*, values of *p* were calculated using Student's t test). (**G,H**) Analyzed by qRT-PCR and immunostainings (scale bars 25 µm), *Arnt* over-expression ($Arnt^{oe}$) was assessed (n=3 independent experiments, data are presented as means±s.d., **** *p<0.0001*, values of *p* were calculated using Student's t test). (**I-L**) TECs were transfected with either scrambled RNA (*scrRNA*), siRNA targeting Hif1α ($Hif1a^{kd}$) or Ahr (Ahr^{kd}). Analyzed by qRT-PCR, the bar graphs summarize relative mRNA expression levels of respective transcripts in response to either FK506 (200 pM) or transgenic Arnt over-expression ($Arnt^{oe}$, n=3 independent experiments, data are presented as means±s.d., # *no significance*, values of *p* were calculated using Student's t test).

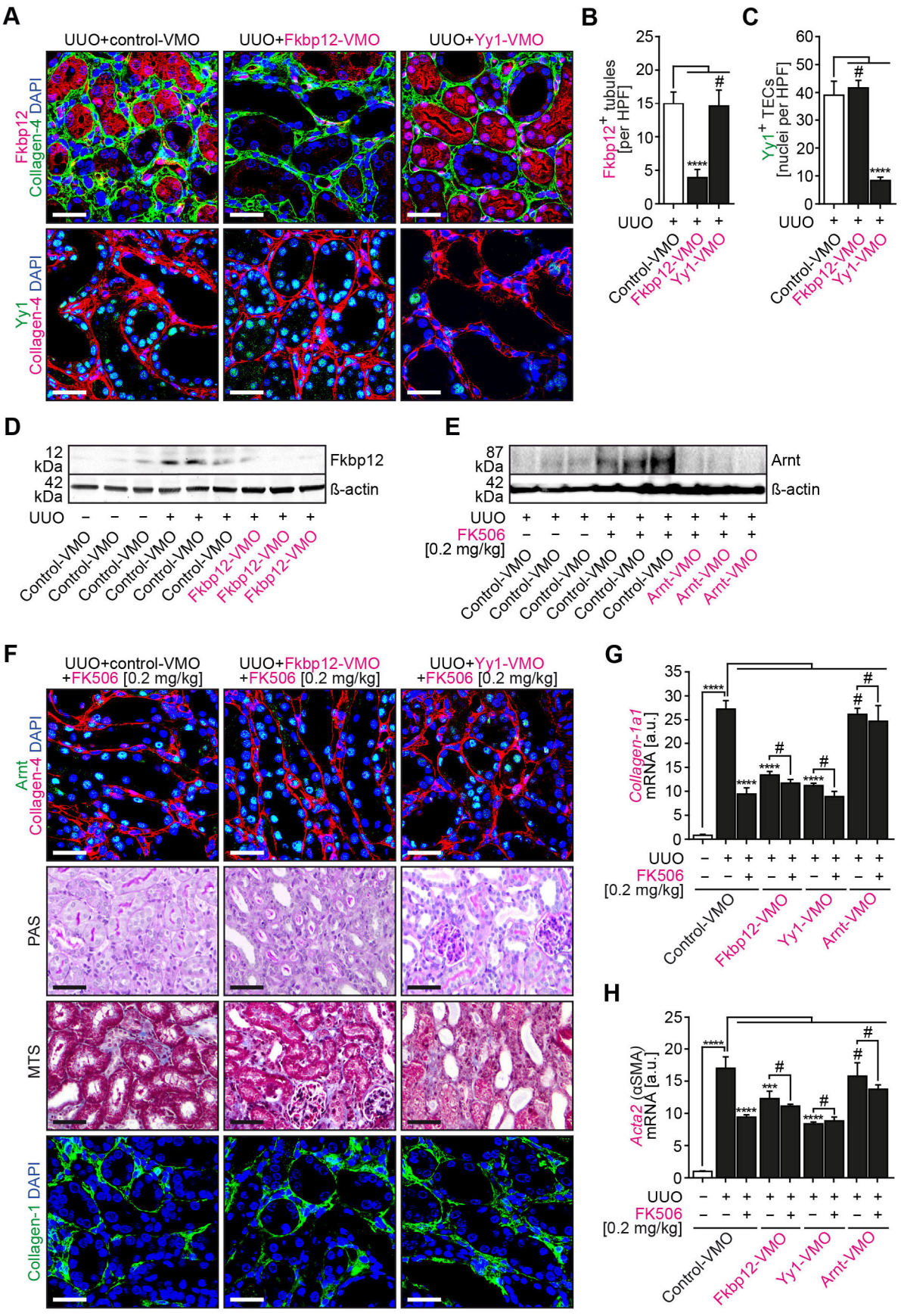

Supplementary Figure 6. (**A-C**) As determined by immunostaining, intrarenal Fkbp12 (scale bars 25 µm) and Yy1 (scale bars 25 µm) were assessed (n=6/group, data are presented as means±s.d., **** *p<0.0001*, # *no significance*, values of *p* were calculated using one-way ANOVA with Bonferroni post-hoc analysis). (**D,E**) Intrarenal Fkbp12 and Arnt were analyzed by immunoblotting of total kidney lysates. (**F**) Representative photomicrographs of kidney sections immunolabelled for Arnt (scale bars 25 µm), PAS (scale bars 50 µm), MTS (scale bars 50 µm) or Collagen-1 (scale bars 25 µm) are shown. (**G,H**) Expression levels of *Collagen-1a1* and *Acta2* (encoding αSMA) were assessed by qRT-PCR (n=3-4/group, data are presented as means±s.d., *** *p<0.001*, **** *p<0.0001*, # *no significance*, values of *p* were calculated using one-way ANOVA with Bonferroni post-hoc analysis).

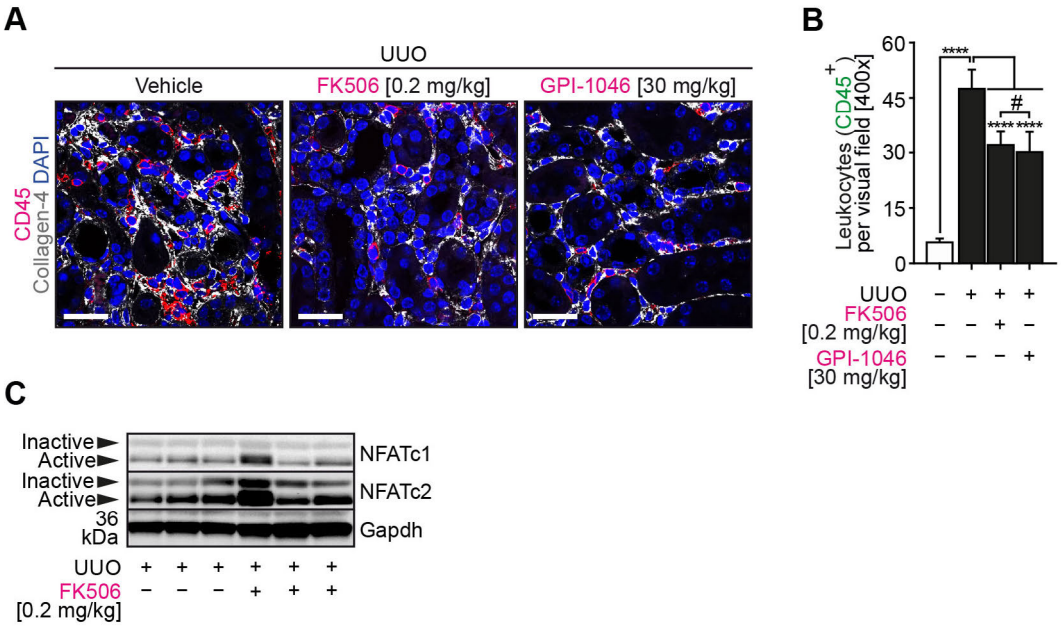

Supplementary Figure 7. (**A,B**) Mice were challenged with UUO and treated with either vehicle buffer, FK506 (0.2 mg/kg orally per day) or GPI-1046 (30 mg/kg orally per day) starting one day prior of UUO surgery, representative kidney sections immunolabbeled with CD45 (scale bars 25 µm) are shown (n=6/group, data are presented as means±s.d., **** *p<0.0001*, # *no significance*, values of *p* were calculated using one-way ANOVA with Bonferroni post-hoc analysis). (**C**) Intrarenal NFATc1 and NFATc2 were assessed by immunoblotting.

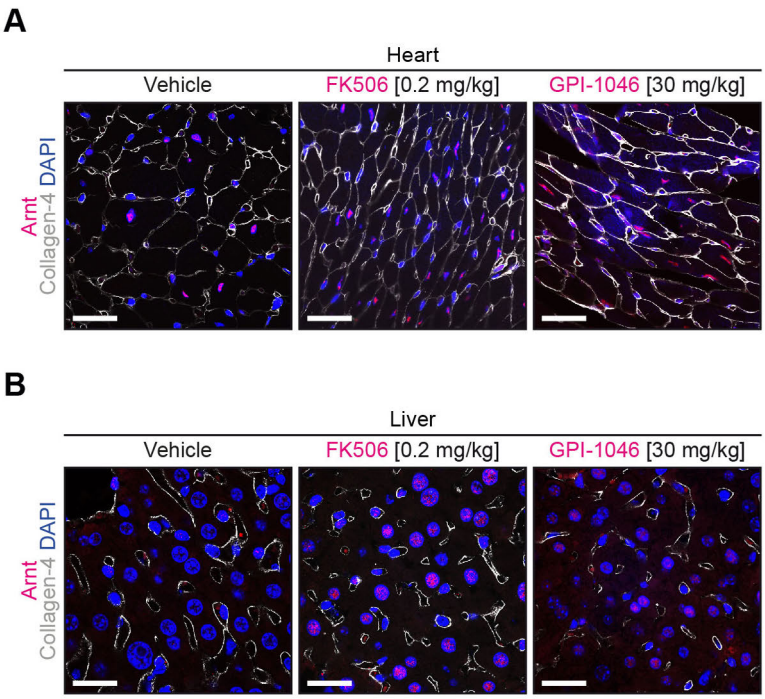

Supplementary Figure 8. (**A,B**) Representative photomicrographs of sections immunolabelled for Arnt (scale bars 25 μm) in hearts and livers of mice administered FK506 or GPI-1046 (0.2 mg/kg or 30 mg/kg orally per day, respectively) are shown.

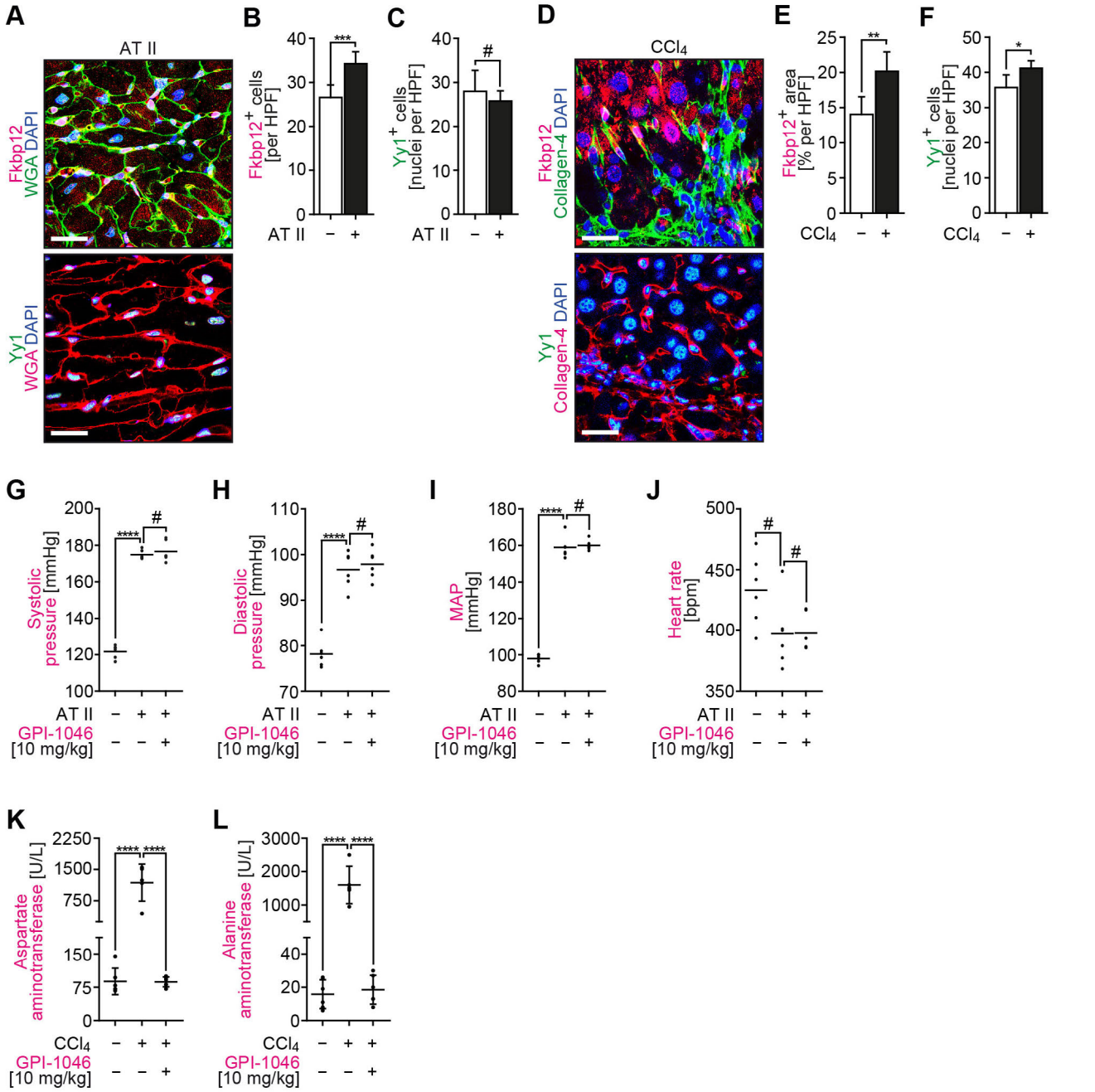

Supplementary Figure 9. (**A-F**) Abundance of Fkbp12 and Yy1 was analyzed by immunostaining (scale bars 25 µm) in AT II-induced cardiomyopathy and CCl_4-mediated liver injury (n=5-7/group, data are presented as means±s.d., * *p<0.05*, ** *p<0.01*, *** *p<0.001*, # *no significance*, values of *p* were calculated using Student's t test). (**G-J**) Systolic, diastolic, mean arterial pressure (MAP) and heart rate beats per minute (BPM) of mice treated with GPI-1046 (10 mg/kg subcutaneously per day) and challenged with AT II are shown (n=6/group, data are presented as aligned dot plots with means±s.d., **** *p<0.0001*, # *no significance*, values of *p* were calculated using one-way ANOVA with Bonferroni post-hoc analysis comparing indicated pairs of columns). (**K,L**) Measurements of aspartate and alanine aminotransferases in mice challenged with CCl_4 are shown (n=5-6/group, data are presented as aligned dot plots with means±s.d., **** *p<0.0001*, values of *p* were calculated using one-way ANOVA with Bonferroni post-hoc analysis).

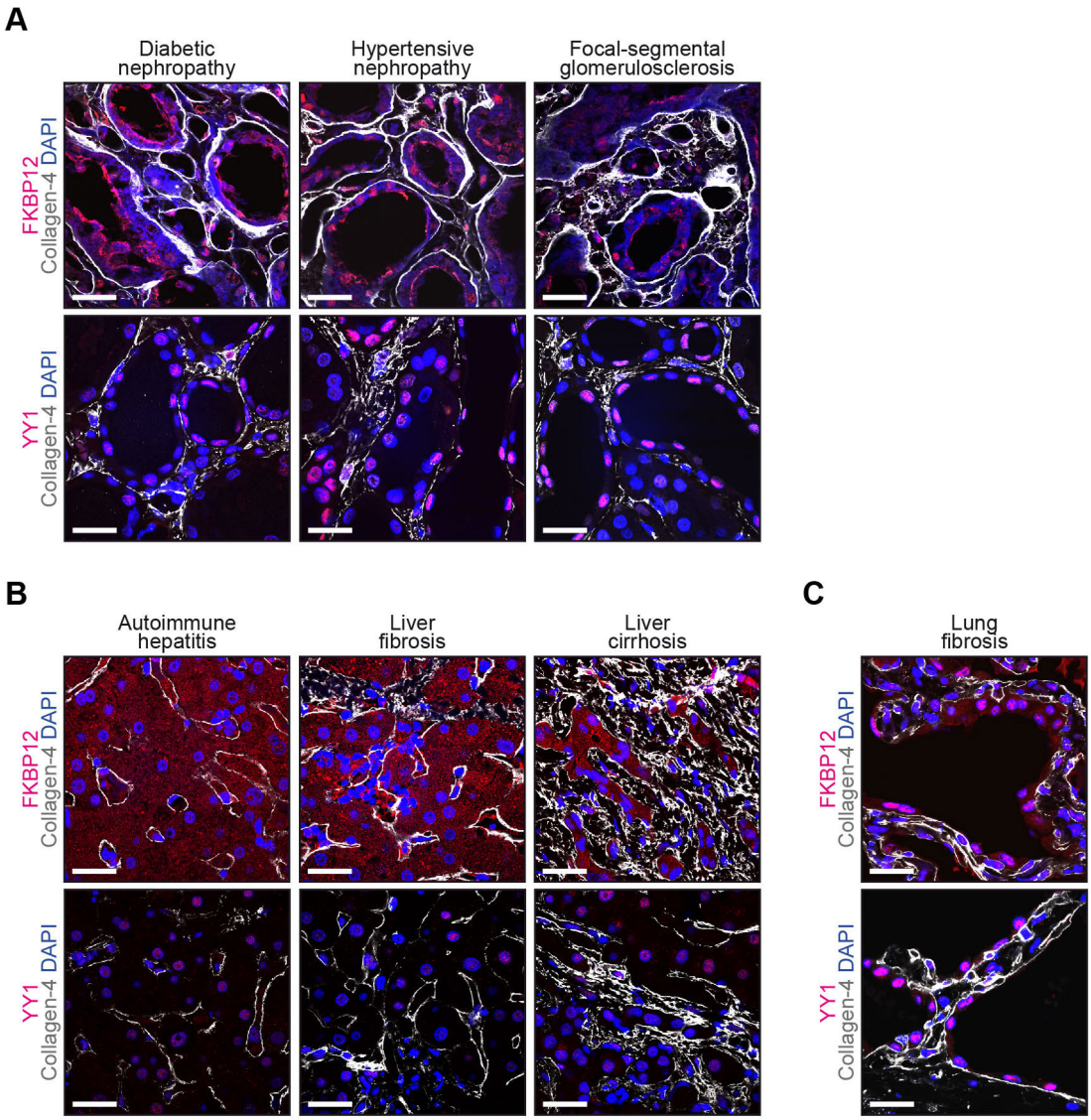

Supplementary Figure 10. (**A-C**) Representative photomicrographs of immunostainings for FKBP12 (scale bars 25 µm) and YY1 (scale bars 25 µm) among different human pathologies are shown.

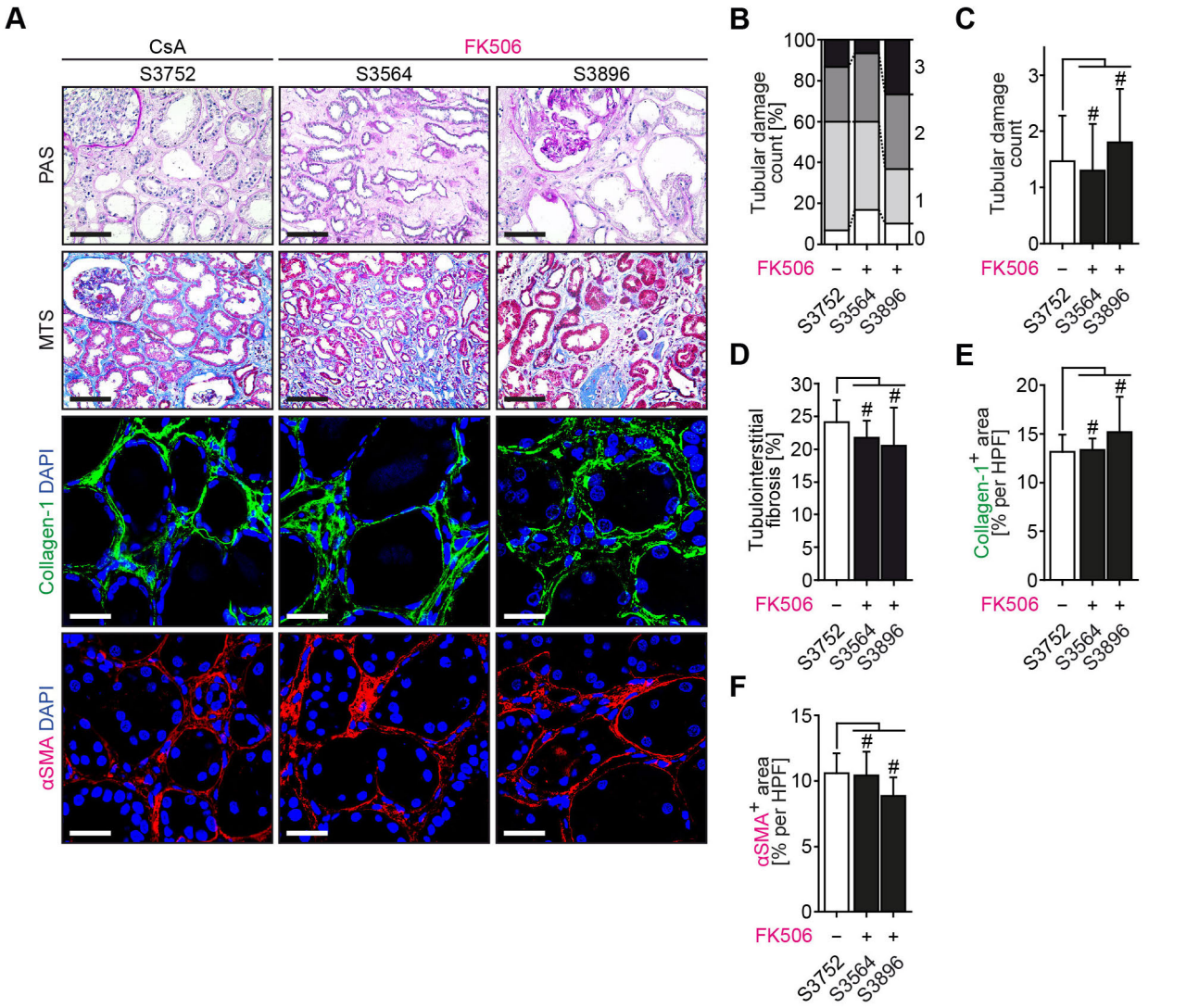

Supplementary Figure 11. (**A-F**) In a small cohort of kidney transplant recipients with comparable histological patterns and immunosuppressive regimens including either CsA or FK506, representative photomicrographs of kidney sections stained for PAS (scale bars 100 µm), MTS (scale bars 100 µm), immunolabelled for Collagen-1 (scale bars 25 µm) or αSMA (scale bars 25 µm) are shown (measurements were done in 10 visual fields, data are presented as means±s.d., *# no significance*, values of *p* were calculated using one-way ANOVA with Bonferroni post-hoc analysis).

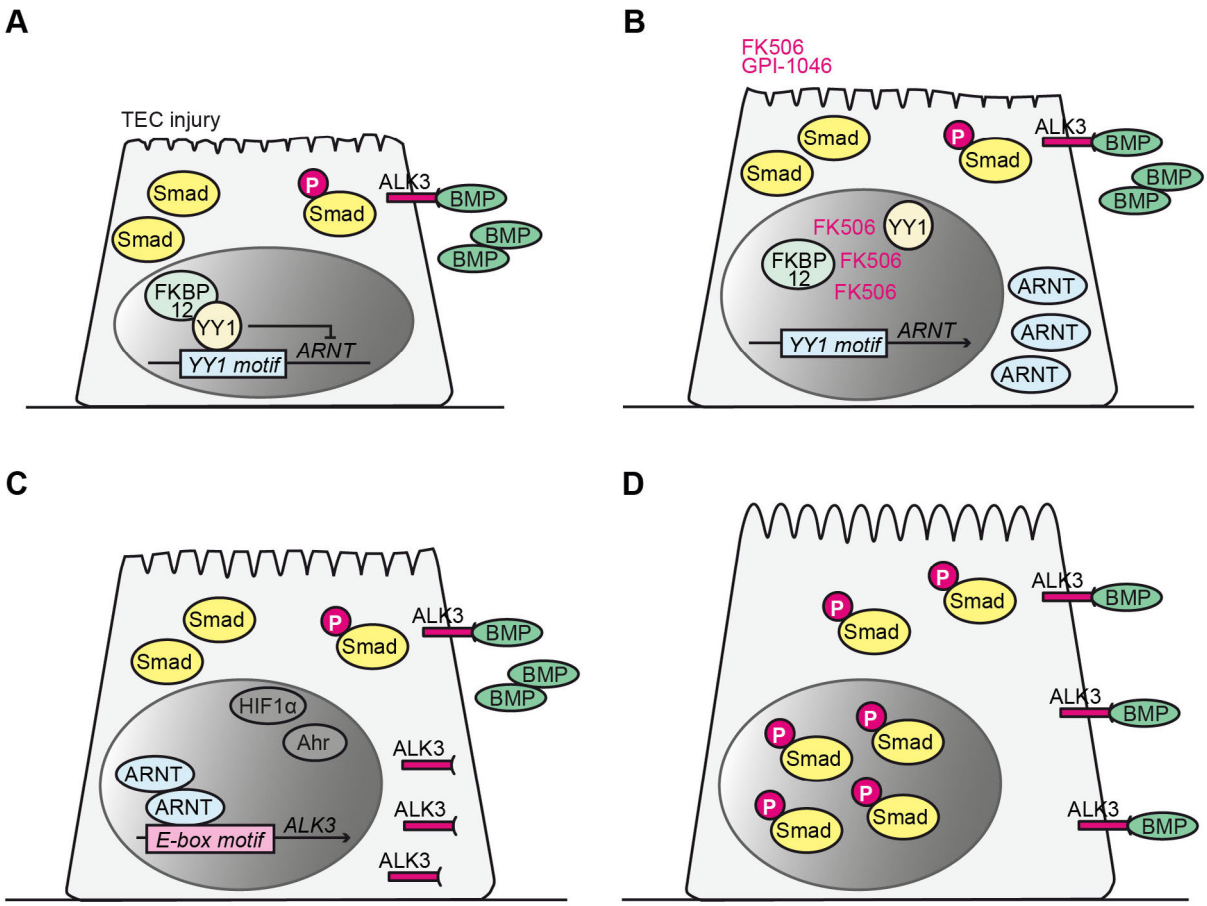

Supplementary Figure 12. (**A**) In injured TECs, FKBP12/YY1 complexes repress *ARNT*. (**B**) FK506 or GPI-1046 disrupt FKBP12/YY1 interaction, in turn associated with release from transcriptional repression of *ARNT*. (**C**) ARNT subsequently mediates transcriptional *ALK3* induction independent of HIF1α or AHR. (**D**) Transcriptional ALK3 induction is associated with activation of canonical BMP signaling responses reflected by nuclear translocation of phosphorylated Smad1/5/8.

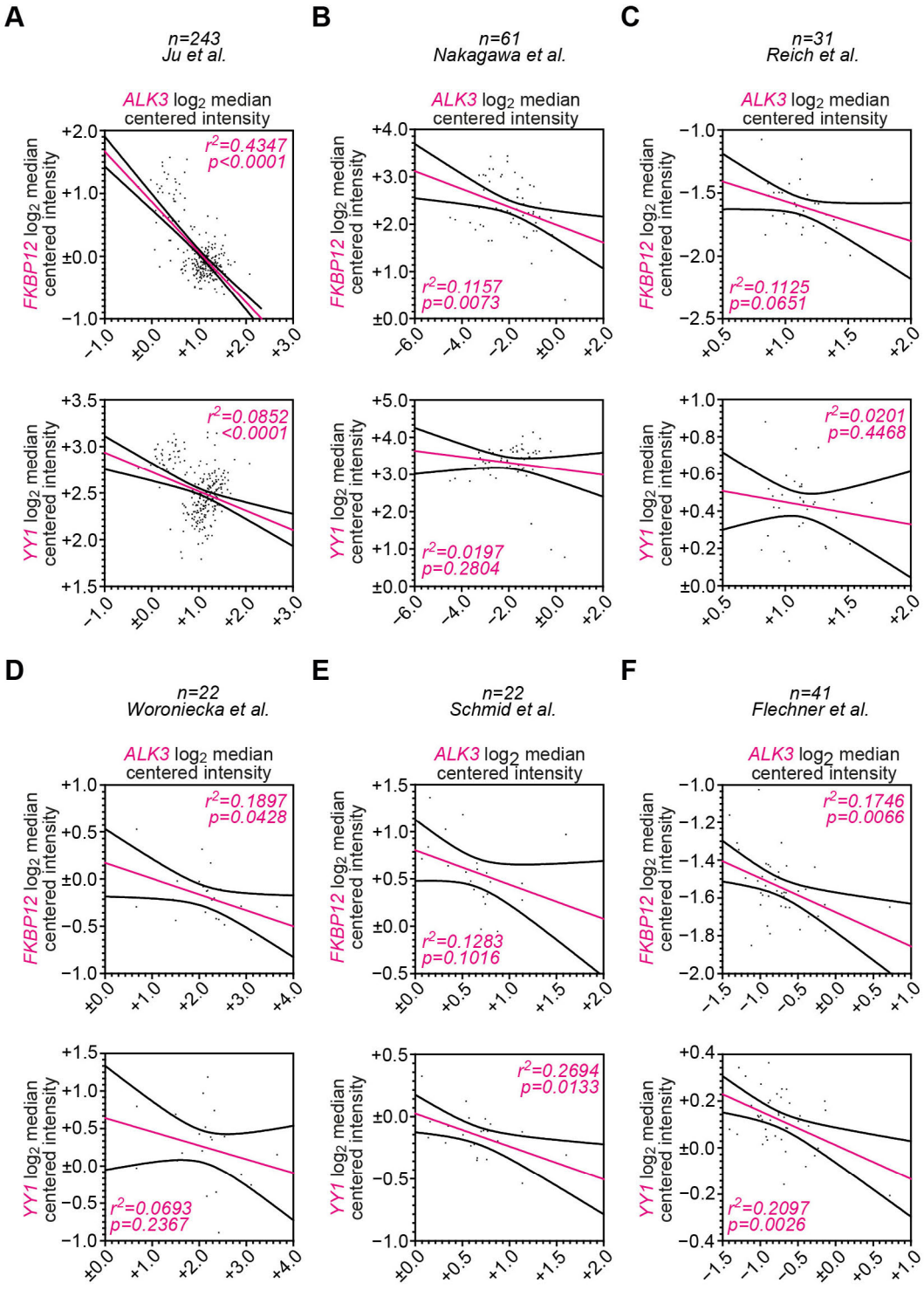

Supplementary Figure 13. (**A-F**) In publicly available datasets, intrarenal *ALK3* expression is inversely correlated with expression levels of *FKBP12* and *YY1* among various kidney pathologies (accession numbers GSE69438 and GSE66494, **A,B**), microdissected tubulointerstitial compartments of IgA nephropathy (accession number GSE35487, **C**), diabetic nephropathy (accession number GSE30566, **D**), in total kidneys of diabetic nephropathy (accession number GSE21785, **E**) and transplant specimens (accession number GSE1563, **F**, n of patients and references are indicated above, data are presented as correlation analyses of $\log_2$ median centered intensity, r^2 and values of p were calculated by linear regression are indicated in the corresponding correlation graphs).

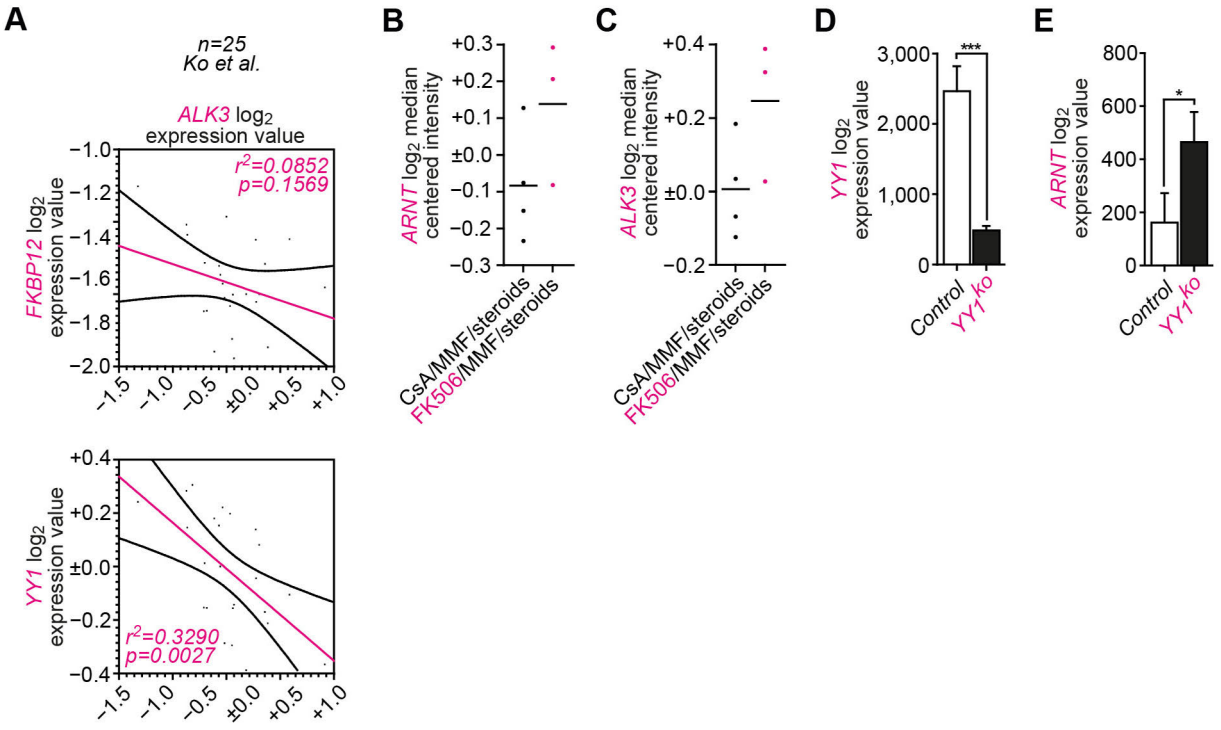

Supplementary Figure 14. (**A**) Inverse coorelation between intrarenal *ALK3* and *FKBP12/YY1* expression levels was confirmed in microdissected renal tubules from diseased kidneys (accession number GSE48944, n of patients and references are indicated above, data are presented as correlation analyses of log_2 expression values, r^2 and values of *p* were calculated by linear regression are indicated in the corresponding correlation graphs). (**B,C**) Compared to regimens including CsA, immunosuppression with FK506 is associated with intrarenal *ARNT* and *ALK3* induction (references are indicated above, data are presented as aligned dot plots of log_2 median centered intensities with means). (**D,E**) Transcriptome array datasets performed in HeLa cells confirmed transcriptional *ARNT* induction when YY1 was depleted (accession number GSE14964, n of replicates as indicated, data are presented as means±s.d. of log_2 expression values, * $p<0.05$, *** $p<0.001$, values of *p* were calculated using Student's t test comparing indicated pairs of columns).

GO term	**description**	**enrichment**	***p* value**
GO:2000404	regulation of T cell migration	61.20	$4.81e^{-4}$
GO:2000406	positive regulation of T cell migration	61.20	$4.81e^{-4}$
GO:2000403	positive regulation of lymphocyte migration	61.20	$4.81e^{-4}$
GO:1900025	negative regulation of substrate adhesion-dependent cell spreading	43.71	$9.73e^{-4}$
GO:0000060	protein import into nucleus, translocation	14.23	$5.27e^{-4}$
GO:0071772	response to BMP	12.24	$8.99e^{-4}$
GO:0071773	cellular response to BMP stimulus	12.24	$8.99e^{-4}$
GO:0035023	regulation of Rho protein signal transduction	10.41	$3.83e^{-4}$
GO:0043547	positive regulation of GTPase activity	8.63	$9.17e^{-6}$
GO:0046578	regulation of Ras protein signal transduction	8.33	$3.14e^{-4}$
GO:0051056	regulation of small GTPase mediated signaling transduction	7.85	$1.09e^{-4}$
GO:0043087	regulation of GTPase activity	7.77	$2.50e^{-5}$
GO:0044236	multicellular organismal metabolic process	4,54	$2.76e^{-4}$
GO:0044763	single-organism cellular process	1.02	$7.32e^{-4}$

Supplementary Table 1. Pathway analysis in response to FK506 (accession number GSE5258).

transcription factor	association score	*p* value
E2F-1/E2F-2	6.747	$1.30e^{-5}$
C-ETS-1	6.450	$2.70e^{-5}$
MAZ	5.380	$2.43e^{-4}$
MAX	5.380	$2.43e^{-4}$
E2F-1	4.705	$1.01e^{-3}$
TFII-I	4.593	$1.34e^{-3}$
SPZ1	4.557	$1.45e^{-3}$
AP-2	4.460	$1.75e^{-3}$
PAX-5	4.344	$2.22e^{-3}$
MAZR	4.254	$2.71e^{-3}$
USF1	4.201	$2.94e^{-3}$
EGR-1/EGR-2	4.139	$3.20e^{-3}$
PEA3	3.950	$4.92e^{-3}$
ATF6	3.887	$5.72e^{-3}$
ARNT	3.823	$6.58e^{-3}$
SP1	3.785	$6.93e^{-3}$
SP1/SP3	3.778	$7.02e^{-3}$
SP1/SP2	3.777	$7.04e^{-3}$
YY1	3.776	$7.06e^{-3}$
STRA13	3.762	$7.31e^{-3}$
AHR/ARNT	3.725	$7.89e^{-3}$
PAX-9A	3.719	$7.95e^{-3}$
RELA	3.638	$9.37e^{-3}$
ATF-1/ATF-2	3.524	$1.15e^{-2}$
MAX	3.519	$1.17e^{-2}$
C-MAF	3.509	$1.17e^{-2}$
ATF3	3.465	$1.29e^{-2}$
TEL-2α/TEL-2β	3.457	$1.32e^{-2}$
n-MYC	3.435	$1.38e^{-2}$
DP-1/E2F-1	3.422	$1.44e^{-2}$
CHCH	3.368	$1.53e^{-2}$
MOVO-β	3.363	$1.56e^{-2}$
NERF-1α	3.304	$1.76e^{-2}$
USF1	3.272	$1.93e^{-2}$
NF-κB1/NF-κB2	3.191	$2.28e^{-2}$
SREBP-1	3.178	$2.36e^{-2}$
ELF-1	3.146	$2.50e^{-2}$
CREB/CREB-β	3.101	$2.61e^{-2}$
BRCA1	3.085	$2.67e^{-2}$
NRF-1	3.076	$2.70e^{-2}$
ZF5	3.070	$2.75e^{-2}$
HIF-1α	2.996	$3.31e^{-2}$
USF1	2.989	$3.36e^{-2}$
CREB	2.989	$3.36e^{-2}$
GABP-α/GABP-β1	2.978	$3.43e^{-2}$

AHR	2.954	$3.56e^{-2}$
AP-2α	2.853	$4.25e^{-2}$
ATF4	2.819	$4.54e^{-2}$
EGR-4	2.811	$4.58e^{-2}$
ELK-1	2.780	$4.89e^{-2}$
AP-2γ	2.769	$4.96e^{-2}$

Supplementary Table 2. Motif enrichment analysis of differentially expressed genes induced in response to FK506 (accession number GSE5258).

description	maximal score	total score	query cover	E value	identity	accession
Mus musculus FK506 binding protein 1a (Fkbp1a), transcript variant 3, non-coding RNA	50.1	50.1	100%	3,00E-06	100%	NR_126058.1
Mus musculus FK506 binding protein 1a (Fkbp1a), transcript variant 6, mRNA	50.1	50.1	100%	3,00E-06	100%	NM_001302080.1
Mus musculus FK506 binding protein 1a (Fkbp1a), transcript variant 5, mRNA	50.1	50.1	100%	3,00E-06	100%	NM_001302079.1
Mus musculus FK506 binding protein 1a (Fkbp1a), transcript variant 4, mRNA	50.1	50.1	100%	3,00E-06	100%	NM_001302078.1
Mus musculus FK506 binding protein 1a (Fkbp1a), transcript variant 2, mRNA	50.1	50.1	100%	3,00E-06	100%	NM_001302077.1
Mus musculus FK506 binding protein 1a (Fkbp1a), transcript variant 1, mRNA	50.1	50.1	100%	3,00E-06	100%	NM_008019.3
PREDICTED: Mus musculus pregnancy specific glycoprotein 19 (Psg19), transcript variant X1, mRNA	32.2	32.2	64%	0.65	100%	XM_006540007.3
PREDICTED: Mus musculus pregnancy-specific glycoprotein 22 (Psg22), transcript variant X1, mRNA	32.2	32.2	64%	0.65	100%	XM_017322233.1
Mus musculus pregnancy-specific glycoprotein 22 (Psg22), mRNA	32.2	32.2	64%	0.65	100%	NM_001004152.2
Mus musculus pregnancy specific glycoprotein 19 (Psg19), mRNA	32.2	32.2	64%	0.65	100%	NM_011964.2
Mus musculus aminolevulinic acid synthase 2, erythroid (Alas2), transcript variant 2, mRNA	32.2	32.2	64%	0.65	100%	NM_001102446.1
Mus musculus aminolevulinic acid synthase 2, erythroid (Alas2), transcript variant 1, mRNA	32.2	32.2	64%	0.65	100%	NM_009653.3
PREDICTED: Mus musculus NHS-like 2 (Nhsl2), transcript variant X4, mRNA	30.2	30.2	76%	2.6	95%	XM_006527721.3
PREDICTED: Mus musculus dynamin 2 (Dnm2), transcript variant X18, mRNA	30.2	30.2	60%	2.6	100%	XM_006509985.3
PREDICTED: Mus musculus dynamin 2 (Dnm2), transcript variant X15, mRNA	30.2	30.2	60%	2.6	100%	XM_017313129.1
PREDICTED: Mus musculus dynamin 2 (Dnm2), transcript variant X14, mRNA	30.2	30.2	60%	2.6	100%	XM_006509982.2
PREDICTED: Mus musculus dynamin 2 (Dnm2), transcript variant X13, mRNA	30.2	30.2	60%	2.6	100%	XM_006509981.2
PREDICTED: Mus musculus dynamin 2 (Dnm2), transcript variant X12, mRNA	30.2	30.2	60%	2.6	100%	XM_017313128.1
PREDICTED: Mus musculus dynamin 2 (Dnm2), transcript variant X11, mRNA	30.2	30.2	60%	2.6	100%	XM_017313127.1
PREDICTED: Mus musculus dynamin 2 (Dnm2), transcript variant X10, mRNA	30.2	30.2	60%	2.6	100%	XM_017313126.1
PREDICTED: Mus musculus dynamin 2 (Dnm2), transcript variant X9, mRNA	30.2	30.2	60%	2.6	100%	XM_006509980.2
PREDICTED: Mus musculus dynamin 2 (Dnm2), transcript variant X7, mRNA	30.2	30.2	60%	2.6	100%	XM_006509978.2
PREDICTED: Mus musculus dynamin 2 (Dnm2), transcript variant X5, mRNA	30.2	30.2	60%	2.6	100%	XM_017313125.1
PREDICTED: Mus musculus dynamin 2 (Dnm2), transcript variant X4, mRNA	30.2	30.2	60%	2.6	100%	XM_006509976.2
PREDICTED: Mus musculus discs, large (Drosophila) homolog-associated protein 3 (Dlgap3), transcript variant X3, mRNA	30.2	30.2	76%	2.6	95%	XM_006503105.3
PREDICTED: Mus musculus discs, large (Drosophila) homolog-associated protein 3 (Dlgap3), transcript variant X2, mRNA	30.2	30.2	76%	2.6	95%	XM_006503104.3
PREDICTED: Mus musculus discs, large (Drosophila) homolog-associated protein 3 (Dlgap3), transcript variant X1, mRNA	30.2	30.2	76%	2.6	95%	XM_011240537.2
PREDICTED: Mus musculus dynamin 1 (Dnm1), transcript variant X18, misc_RNA	30.2	30.2	60%	2.6	100%	XR_374058.3
PREDICTED: Mus musculus dynamin 1 (Dnm1), transcript variant X16, misc_RNA	30.2	30.2	60%	2.6	100%	XR_001780678.1
PREDICTED: Mus musculus dynamin 1 (Dnm1), transcript variant X15, misc_RNA	30.2	30.2	60%	2.6	100%	XR_001780675.1
PREDICTED: Mus musculus dynamin 1 (Dnm1), transcript variant X10, mRNA	30.2	30.2	60%	2.6	100%	XM_017315328.1
PREDICTED: Mus musculus dynamin 1 (Dnm1), transcript variant X9, mRNA	30.2	30.2	60%	2.6	100%	XM_006497659.3
PREDICTED: Mus musculus dynamin 1 (Dnm1), transcript variant X8, mRNA	30.2	30.2	60%	2.6	100%	XM_006497658.3
PREDICTED: Mus musculus dynamin 1 (Dnm1), transcript variant X5, mRNA	30.2	30.2	60%	2.6	100%	XM_006497654.3
PREDICTED: Mus musculus tripartite motif-containing 9 (Trim9), transcript variant X12, mRNA	30.2	30.2	60%	2.6	100%	XM_006516407.3

PREDICTED: Mus musculus tripartite motif-containing 9 (Trim9), transcript variant X11, misc_RNA	30.2	30.2	60%	2.6	100%	XR_381560.3
PREDICTED: Mus musculus tripartite motif-containing 9 (Trim9), transcript variant X10, mRNA	30.2	30.2	60%	2.6	100%	XM_006516406.3
PREDICTED: Mus musculus tripartite motif-containing 9 (Trim9), transcript variant X9, mRNA	30.2	30.2	60%	2.6	100%	XM_006516405.3
PREDICTED: Mus musculus tripartite motif-containing 9 (Trim9), transcript variant X8, mRNA	30.2	30.2	60%	2.6	100%	XM_006516404.3
PREDICTED: Mus musculus tripartite motif-containing 9 (Trim9), transcript variant X7, mRNA	30.2	30.2	60%	2.6	100%	XM_006516403.3
PREDICTED: Mus musculus tripartite motif-containing 9 (Trim9), transcript variant X6, mRNA	30.2	30.2	60%	2.6	100%	XM_006516402.3
PREDICTED: Mus musculus tripartite motif-containing 9 (Trim9), transcript variant X5, mRNA	30.2	30.2	60%	2.6	100%	XM_017315265.1
PREDICTED: Mus musculus tripartite motif-containing 9 (Trim9), transcript variant X4, mRNA	30.2	30.2	60%	2.6	100%	XM_017315264.1
PREDICTED: Mus musculus tripartite motif-containing 9 (Trim9), transcript variant X3, mRNA	30.2	30.2	60%	2.6	100%	XM_006516401.3
PREDICTED: Mus musculus tripartite motif-containing 9 (Trim9), transcript variant X2, mRNA	30.2	30.2	60%	2.6	100%	XM_017315263.1
PREDICTED: Mus musculus tripartite motif-containing 9 (Trim9), transcript variant X1, mRNA	30.2	30.2	60%	2.6	100%	XM_006516400.3
PREDICTED: Mus musculus armadillo repeat containing 9 (Armc9), transcript variant X11, mRNA	30.2	52.5	96%	2.6	91%	XM_006529960.3
PREDICTED: Mus musculus dynamin 1 (Dnm1), transcript variant X17, misc_RNA	30.2	30.2	60%	2.6	100%	XR_374057.2
PREDICTED: Mus musculus dynamin 1 (Dnm1), transcript variant X14, misc_RNA	30.2	30.2	60%	2.6	100%	XR_374055.2
PREDICTED: Mus musculus dynamin 1 (Dnm1), transcript variant X13, mRNA	30.2	30.2	60%	2.6	100%	XM_006497662.2
PREDICTED: Mus musculus dynamin 1 (Dnm1), transcript variant X12, mRNA	30.2	30.2	60%	2.6	100%	XM_006497661.2
PREDICTED: Mus musculus dynamin 1 (Dnm1), transcript variant X11, mRNA	30.2	30.2	60%	2.6	100%	XM_006497660.2
PREDICTED: Mus musculus dynamin 1 (Dnm1), transcript variant X7, mRNA	30.2	30.2	60%	2.6	100%	XM_006497653.2
PREDICTED: Mus musculus dynamin 1 (Dnm1), transcript variant X6, mRNA	30.2	30.2	60%	2.6	100%	XM_006497655.2
PREDICTED: Mus musculus dynamin 1 (Dnm1), transcript variant X4, mRNA	30.2	30.2	60%	2.6	100%	XM_006497652.2
PREDICTED: Mus musculus dynamin 1 (Dnm1), transcript variant X3, mRNA	30.2	30.2	60%	2.6	100%	XM_006497651.2
PREDICTED: Mus musculus dynamin 1 (Dnm1), transcript variant X2, mRNA	30.2	30.2	60%	2.6	100%	XM_006497650.2
PREDICTED: Mus musculus dynamin 1 (Dnm1), transcript variant X1, mRNA	30.2	30.2	60%	2.6	100%	XM_006497649.2
Mus musculus discs, large (Drosophila) homolog-associated protein 3 (Dlgap3), transcript variant 2, mRNA	30.2	30.2	76%	2.6	95%	NM_001302081.1
Mus musculus discs, large (Drosophila) homolog-associated protein 3 (Dlgap3), transcript variant 1, mRNA	30.2	30.2	76%	2.6	95%	NM_198618.5
Mus musculus dynamin 1 (Dnm1), transcript variant 3, non-coding RNA	30.2	30.2	60%	2.6	100%	NR_125959.1
Mus musculus dynamin 1 (Dnm1), transcript variant 2, mRNA	30.2	30.2	60%	2.6	100%	NM_001301737.1
Mus musculus dynamin 1 (Dnm1), transcript variant 1, mRNA	30.2	30.2	60%	2.6	100%	NM_010065.3
PREDICTED: Mus musculus dynamin 2 (Dnm2), transcript variant X16, mRNA	30.2	30.2	60%	2.6	100%	XM_006509983.1
PREDICTED: Mus musculus dynamin 2 (Dnm2), transcript variant X8, mRNA	30.2	30.2	60%	2.6	100%	XM_006509979.1
PREDICTED: Mus musculus dynamin 2 (Dnm2), transcript variant X6, mRNA	30.2	30.2	60%	2.6	100%	XM_006509977.1
PREDICTED: Mus musculus dynamin 2 (Dnm2), transcript variant X3, mRNA	30.2	30.2	60%	2.6	100%	XM_006509975.1
PREDICTED: Mus musculus dynamin 2 (Dnm2), transcript variant X2, mRNA	30.2	30.2	60%	2.6	100%	XM_006509974.1
PREDICTED: Mus musculus dynamin 2 (Dnm2), transcript variant X1, mRNA	30.2	30.2	60%	2.6	100%	XM_006509973.1
PREDICTED: Mus musculus fat mass and obesity associated (Fto), transcript variant X1, mRNA	30.2	30.2	60%	2.6	100%	XM_006531036.1
Mus musculus tripartite motif-containing 9 (Trim9), transcript variant 6, mRNA	30.2	30.2	60%	2.6	100%	NM_001286388.1

Mus musculus tripartite motif-containing 9 (Trim9), transcript variant 5, mRNA	30.2	30.2	60%	2.6	100%	NM_001286387.1
Mus musculus tripartite motif-containing 9 (Trim9), transcript variant 4, mRNA	30.2	30.2	60%	2.6	100%	NM_001286386.1
Mus musculus dynamin 2 (Dnm2), transcript variant 4, mRNA	30.2	30.2	60%	2.6	100%	NM_001253894.1
Mus musculus dynamin 2 (Dnm2), transcript variant 3, mRNA	30.2	30.2	60%	2.6	100%	NM_007871.2
Mus musculus dynamin 2 (Dnm2), transcript variant 2, mRNA	30.2	30.2	60%	2.6	100%	NM_001039520.2
Mus musculus dynamin 2 (Dnm2), transcript variant 1, mRNA	30.2	30.2	60%	2.6	100%	NM_001253893.1
Mus musculus fat mass and obesity associated (Fto), mRNA	30.2	30.2	60%	2.6	100%	NM_011936.2
Mus musculus tripartite motif-containing 9 (Trim9), transcript variant 3, mRNA	30.2	30.2	60%	2.6	100%	NM_001110203.1
Mus musculus tripartite motif-containing 9 (Trim9), transcript variant 2, mRNA	30.2	30.2	60%	2.6	100%	NM_001110202.1
Mus musculus tripartite motif-containing 9 (Trim9), transcript variant 1, mRNA	30.2	30.2	60%	2.6	100%	NM_053167.3
Mus musculus WAP, FS, Ig, KU, and NTR-containing protein 1 (Wfikkn1), mRNA	30.2	30.2	60%	2.6	100%	NM_001100454.1
PREDICTED: Mus musculus intestinal cell kinase (Ick), transcript variant X2, mRNA	28.2	28.2	56%	10	100%	XM_006511305.3
PREDICTED: Mus musculus hydroxysteroid dehydrogenase like 1 (Hsdl1), transcript variant X7, misc_RNA	28.2	28.2	56%	10	100%	XR_001778478.1
PREDICTED: Mus musculus hydroxysteroid dehydrogenase like 1 (Hsdl1), transcript variant X4, mRNA	28.2	28.2	56%	10	100%	XM_006531397.3
PREDICTED: Mus musculus hydroxysteroid dehydrogenase like 1 (Hsdl1), transcript variant X3, mRNA	28.2	28.2	56%	10	100%	XM_006531395.3
PREDICTED: Mus musculus hydroxysteroid dehydrogenase like 1 (Hsdl1), transcript variant X2, mRNA	28.2	28.2	56%	10	100%	XM_006531394.3
PREDICTED: Mus musculus hydroxysteroid dehydrogenase like 1 (Hsdl1), transcript variant X1, mRNA	28.2	28.2	56%	10	100%	XM_006531393.3
PREDICTED: Mus musculus kinesin family member C3 (Kifc3), transcript variant X7, mRNA	28.2	28.2	56%	10	100%	XM_017312585.1
PREDICTED: Mus musculus kinesin family member C3 (Kifc3), transcript variant X6, mRNA	28.2	28.2	56%	10	100%	XM_006530723.3
PREDICTED: Mus musculus uncharacterized LOC108167423 (LOC108167423), transcript variant X2, ncRNA	28.2	28.2	56%	10	100%	XR_001778116.1
PREDICTED: Mus musculus uncharacterized LOC108167423 (LOC108167423), transcript variant X1, ncRNA	28.2	28.2	56%	10	100%	XR_001778115.1
PREDICTED: Mus musculus IQ motif containing GTPase activating protein 1 (Iqgap1), transcript variant X3, misc_RNA	28.2	52.5	80%	10	100%	XR_001785567.1
PREDICTED: Mus musculus IQ motif containing GTPase activating protein 1 (Iqgap1), transcript variant X2, misc_RNA	28.2	28.2	56%	10	100%	XR_391347.3
PREDICTED: Mus musculus IQ motif containing GTPase activating protein 1 (Iqgap1), transcript variant X1, mRNA	28.2	52.5	80%	10	100%	XM_006540950.3
PREDICTED: Mus musculus chloride channel, voltage-sensitive 1 (Clcn1), transcript variant X3, mRNA	28.2	28.2	56%	10	100%	XM_006505477.3
PREDICTED: Mus musculus adrenergic receptor kinase, beta 2 (Adrbk2), transcript variant X3, misc_RNA	28.2	28.2	56%	10	100%	XR_880393.2
PREDICTED: Mus musculus adrenergic receptor kinase, beta 2 (Adrbk2), transcript variant X1, misc_RNA	28.2	28.2	56%	10	100%	XR_389274.3
PREDICTED: Mus musculus predicted gene 15800 (Gm15800), transcript variant X11, mRNA	28.2	50.5	76%	10	100%	XM_006530360.3
PREDICTED: Mus musculus predicted gene 15800 (Gm15800), transcript variant X10, mRNA	28.2	28.2	56%	10	100%	XM_006530359.3

Supplementary Table 3. Sequence alignment of Fkbp12-VMO.

description	maximal score	total score	query cover	E value	identity	accession
PREDICTED: Mus musculus YY1 transcription factor (Yy1), transcript variant X1, mRNA	50.1	50.1	100%	3,00E-06	100%	XM_006515820.3
Mus musculus YY1 transcription factor (Yy1), mRNA	50.1	50.1	100%	3,00E-06	100%	NM_009537.3
PREDICTED: Mus musculus dystonin (Dst), transcript variant X30, mRNA	28.2	28.2	56%	10	100%	XM_006495691.3
PREDICTED: Mus musculus dystonin (Dst), transcript variant X29, mRNA	28.2	28.2	56%	10	100%	XM_006495690.3
PREDICTED: Mus musculus dystonin (Dst), transcript variant X28, mRNA	28.2	28.2	56%	10	100%	XM_017314868.1
PREDICTED: Mus musculus dystonin (Dst), transcript variant X27, mRNA	28.2	28.2	56%	10	100%	XM_006495688.3
PREDICTED: Mus musculus dystonin (Dst), transcript variant X26, mRNA	28.2	28.2	56%	10	100%	XM_017314848.1
PREDICTED: Mus musculus dystonin (Dst), transcript variant X24, mRNA	28.2	28.2	56%	10	100%	XM_006495685.2
PREDICTED: Mus musculus dystonin (Dst), transcript variant X23, mRNA	28.2	28.2	56%	10	100%	XM_006495684.3
PREDICTED: Mus musculus dystonin (Dst), transcript variant X22, mRNA	28.2	28.2	56%	10	100%	XM_017314811.1
PREDICTED: Mus musculus dystonin (Dst), transcript variant X21, mRNA	28.2	28.2	56%	10	100%	XM_006495682.2
PREDICTED: Mus musculus dystonin (Dst), transcript variant X20, mRNA	28.2	28.2	56%	10	100%	XM_017314794.1
PREDICTED: Mus musculus dystonin (Dst), transcript variant X19, mRNA	28.2	28.2	56%	10	100%	XM_006495680.3
PREDICTED: Mus musculus dystonin (Dst), transcript variant X18, mRNA	28.2	28.2	56%	10	100%	XM_006495679.3
PREDICTED: Mus musculus dystonin (Dst), transcript variant X17, mRNA	28.2	28.2	56%	10	100%	XM_006495678.3
PREDICTED: Mus musculus dystonin (Dst), transcript variant X16, mRNA	28.2	28.2	56%	10	100%	XM_017314750.1
PREDICTED: Mus musculus dystonin (Dst), transcript variant X15, mRNA	28.2	28.2	56%	10	100%	XM_017314741.1
PREDICTED: Mus musculus dystonin (Dst), transcript variant X14, mRNA	28.2	28.2	56%	10	100%	XM_006495674.3
PREDICTED: Mus musculus dystonin (Dst), transcript variant X13, mRNA	28.2	28.2	56%	10	100%	XM_017314722.1
PREDICTED: Mus musculus dystonin (Dst), transcript variant X12, mRNA	28.2	28.2	56%	10	100%	XM_017314716.1
PREDICTED: Mus musculus dystonin (Dst), transcript variant X11, mRNA	28.2	28.2	56%	10	100%	XM_017314712.1
PREDICTED: Mus musculus dystonin (Dst), transcript variant X10, mRNA	28.2	28.2	56%	10	100%	XM_017314706.1
PREDICTED: Mus musculus dystonin (Dst), transcript variant X9, mRNA	28.2	28.2	56%	10	100%	XM_006495669.3
PREDICTED: Mus musculus dystonin (Dst), transcript variant X8, mRNA	28.2	28.2	56%	10	100%	XM_017314689.1
PREDICTED: Mus musculus dystonin (Dst), transcript variant X7, mRNA	28.2	28.2	56%	10	100%	XM_017314687.1
PREDICTED: Mus musculus dystonin (Dst), transcript variant X6, mRNA	28.2	28.2	56%	10	100%	XM_017314676.1
PREDICTED: Mus musculus dystonin (Dst), transcript variant X5, mRNA	28.2	28.2	56%	10	100%	XM_017314665.1
PREDICTED: Mus musculus dystonin (Dst), transcript variant X4, mRNA	28.2	28.2	56%	10	100%	XM_017314651.1
PREDICTED: Mus musculus dystonin (Dst), transcript variant X3, mRNA	28.2	28.2	56%	10	100%	XM_006495666.3
PREDICTED: Mus musculus dystonin (Dst), transcript variant X2, mRNA	28.2	28.2	56%	10	100%	XM_017314635.1
PREDICTED: Mus musculus dystonin (Dst), transcript variant X1, mRNA	28.2	28.2	56%	10	100%	XM_017314621.1
Mus musculus active BCR-related gene (Abr), transcript variant 3, mRNA	28.2	28.2	56%	10	100%	NM_198895.2
Mus musculus dystonin (Dst), transcript variant 3, mRNA	28.2	28.2	56%	10	100%	NM_133833.3
Mus musculus dystonin (Dst), transcript variant 2, mRNA	28.2	28.2	56%	10	100%	NM_134448.3
Mus musculus dystonin (Dst), transcript variant 1, mRNA	28.2	28.2	56%	10	100%	NM_001276764.1
Mus musculus insulin-like 3 (Insl3), mRNA	28.2	28.2	56%	10	100%	NM_013564.7
PREDICTED: Mus musculus SREBF chaperone (Scap), transcript variant X3, mRNA	26.3	26.3	52%	40	100%	XM_006512085.3

PREDICTED: Mus musculus SREBF chaperone (Scap), transcript variant X1, mRNA	26.3	26.3	52%	40	100%	XM_006512084.3
PREDICTED: Mus musculus synuclein, alpha interacting protein (synphilin) (Sncaip), transcript variant X2, mRNA	26.3	26.3	52%	40	100%	XM_006526192.3
PREDICTED: Mus musculus HMG box domain containing 3 (Hmgxb3), transcript variant X1, mRNA	26.3	26.3	52%	40	100%	XM_017317779.1
PREDICTED: Mus musculus exocyst complex component 3 (Exoc3), transcript variant X3, mRNA	26.3	26.3	52%	40	100%	XM_017315474.1
PREDICTED: Mus musculus exocyst complex component 3 (Exoc3), transcript variant X1, mRNA	26.3	26.3	52%	40	100%	XM_006517191.2
PREDICTED: Mus musculus SREBF chaperone (Scap), transcript variant X2, mRNA	26.3	26.3	52%	40	100%	XM_006512083.2
Mus musculus SREBF chaperone (Scap), transcript variant 1, mRNA	26.3	26.3	52%	40	100%	NM_001001144.3
Mus musculus SREBF chaperone (Scap), transcript variant 2, mRNA	26.3	26.3	52%	40	100%	NM_001103162.2
Mus musculus forkhead box F1 (Foxf1), mRNA	26.3	26.3	52%	40	100%	NM_010426.2
Mus musculus MARVEL (membrane-associating) domain containing 3 (Marveld3), transcript variant 1, mRNA	26.3	26.3	52%	40	100%	NM_028584.3
Mus musculus MARVEL (membrane-associating) domain containing 3 (Marveld3), transcript variant 2, mRNA	26.3	26.3	52%	40	100%	NM_212447.2
Mus musculus insulinoma-associated 1 (Insm1), mRNA	26.3	26.3	52%	40	100%	NM_016889.3
Mus musculus serine (or cysteine) peptidase inhibitor, clade E, member 1 (Serpine1), mRNA	26.3	26.3	52%	40	100%	NM_008871.2
Mus musculus HMG box domain containing 3 (Hmgxb3), transcript variant 2, mRNA	26.3	26.3	52%	40	100%	NM_134134.2
Mus musculus HMG box domain containing 3 (Hmgxb3), transcript variant 1, mRNA	26.3	26.3	52%	40	100%	NM_178277.1
Mus musculus ATPase, H+ transporting, lysosomal V1 subunit E1 (Atp6v1e1), mRNA	26.3	26.3	52%	40	100%	NM_007510.2
PREDICTED: Mus musculus poly (ADP-ribose) polymerase family, member 3 (Parp3), transcript variant X4, misc_RNA	26.3	26.3	52%	40	100%	XR_001778888.1
PREDICTED: Mus musculus poly (ADP-ribose) polymerase family, member 3 (Parp3), transcript variant X2, mRNA	26.3	26.3	52%	40	100%	XM_006511719.3
PREDICTED: Mus musculus cDNA sequence BC017158 (BC017158), transcript variant X3, mRNA	26.3	26.3	52%	40	100%	XM_011241784.2
PREDICTED: Mus musculus DEAD (Asp-Glu-Ala-Asp) box polypeptide 54 (Ddx54), transcript variant X1, misc_RNA	26.3	26.3	52%	40	100%	XR_878688.2
PREDICTED: Mus musculus actin filament associated protein 1-like 2 (Afap1l2), transcript variant X5, mRNA	26.3	26.3	52%	40	100%	XM_017318171.1
PREDICTED: Mus musculus actin filament associated protein 1-like 2 (Afap1l2), transcript variant X4, mRNA	26.3	26.3	52%	40	100%	XM_017318170.1
PREDICTED: Mus musculus actin filament associated protein 1-like 2 (Afap1l2), transcript variant X2, mRNA	26.3	26.3	52%	40	100%	XM_017318169.1
PREDICTED: Mus musculus actin filament associated protein 1-like 2 (Afap1l2), transcript variant X1, mRNA	26.3	26.3	52%	40	100%	XM_017318168.1
PREDICTED: Mus musculus predicted gene, 31348 (Gm31348), transcript variant X4, ncRNA	26.3	26.3	52%	40	100%	XR_001779509.1
PREDICTED: Mus musculus predicted gene, 31348 (Gm31348), transcript variant X3, ncRNA	26.3	26.3	52%	40	100%	XR_001779508.1
PREDICTED: Mus musculus predicted gene, 31348 (Gm31348), transcript variant X1, ncRNA	26.3	26.3	52%	40	100%	XR_373640.3
Mus musculus poly (ADP-ribose) polymerase family, member 3 (Parp3), transcript variant 1, mRNA	26.3	26.3	52%	40	100%	NM_001311150.1
Mus musculus poly (ADP-ribose) polymerase family, member 3 (Parp3), transcript variant 2, mRNA	26.3	26.3	52%	40	100%	NM_145619.3
PREDICTED: Mus musculus actin filament associated protein 1-like 2 (Afap1l2), transcript variant X3, mRNA	26.3	26.3	52%	40	100%	XM_006527024.2
PREDICTED: Mus musculus poly (ADP-ribose) polymerase family, member 3 (Parp3), transcript variant X3, mRNA	26.3	26.3	52%	40	100%	XM_006511720.1
PREDICTED: Mus musculus poly (ADP-ribose) polymerase family, member 3 (Parp3), transcript variant X1, mRNA	26.3	26.3	52%	40	100%	XM_006511718.1
Mus musculus interleukin-1 receptor-associated kinase 1 (Irak1), transcript variant 1, mRNA	26.3	26.3	68%	40	94%	NM_001177973.1
Mus musculus interleukin-1 receptor-associated kinase 1 (Irak1), transcript variant 3, mRNA	26.3	26.3	68%	40	94%	NM_001177975.1

Mus musculus interleukin-1 receptor-associated kinase 1 (Irak1), transcript variant 2, mRNA	26.3	26.3	68%	40	94%	NM_001177976.1
Mus musculus interleukin-1 receptor-associated kinase 1 (Irak1), transcript variant 5, mRNA	26.3	26.3	68%	40	94%	NM_001177974.1
Mus musculus actin filament associated protein 1-like 2 (Afap1l2), transcript variant 2, mRNA	26.3	26.3	52%	40	100%	NM_001177797.1
Mus musculus actin filament associated protein 1-like 2 (Afap1l2), transcript variant 1, mRNA	26.3	26.3	52%	40	100%	NM_001177796.1
Mus musculus actin filament associated protein 1-like 2 (Afap1l2), transcript variant 3, mRNA	26.3	26.3	52%	40	100%	NM_146102.2
Mus musculus interleukin-1 receptor-associated kinase 1 binding protein 1 (Irak1bp1), transcript variant 2, mRNA	26.3	26.3	68%	40	94%	NM_001168240.1
Mus musculus interleukin-1 receptor-associated kinase 1 binding protein 1 (Irak1bp1), transcript variant 1, mRNA	26.3	26.3	68%	40	94%	NM_022986.4
Mus musculus interleukin-1 receptor-associated kinase 1 (Irak1), transcript variant 4, mRNA	26.3	26.3	68%	40	94%	NM_008363.2
Mus musculus DEAD (Asp-Glu-Ala-Asp) box polypeptide 54 (Ddx54), mRNA	26.3	26.3	52%	40	100%	NM_028041.2
Mus musculus tet methylcytosine dioxygenase 3 (Tet3), transcript variant 1, mRNA	24.3	24.3	48%	159	100%	NM_001347313.1
PREDICTED: Mus musculus RIKEN cDNA C330020E22 gene (C330020E22Rik), transcript variant X13, ncRNA	24.3	24.3	48%	159	100%	XR_390177.3
PREDICTED: Mus musculus RIKEN cDNA C330020E22 gene (C330020E22Rik), transcript variant X12, ncRNA	24.3	24.3	48%	159	100%	XR_882416.2
PREDICTED: Mus musculus RIKEN cDNA C330020E22 gene (C330020E22Rik), transcript variant X11, ncRNA	24.3	24.3	48%	159	100%	XR_882415.2
PREDICTED: Mus musculus RIKEN cDNA C330020E22 gene (C330020E22Rik), transcript variant X5, ncRNA	24.3	24.3	48%	159	100%	XR_882414.2
PREDICTED: Mus musculus RIKEN cDNA C330020E22 gene (C330020E22Rik), transcript variant X10, ncRNA	24.3	24.3	48%	159	100%	XR_882413.2
PREDICTED: Mus musculus coiled-coil domain containing 33 (Ccdc33), transcript variant X8, mRNA	24.3	24.3	48%	159	100%	XM_006511257.3
PREDICTED: Mus musculus coiled-coil domain containing 33 (Ccdc33), transcript variant X7, mRNA	24.3	24.3	48%	159	100%	XM_017313448.1
PREDICTED: Mus musculus coiled-coil domain containing 33 (Ccdc33), transcript variant X6, mRNA	24.3	24.3	48%	159	100%	XM_006511254.3
PREDICTED: Mus musculus coiled-coil domain containing 33 (Ccdc33), transcript variant X5, mRNA	24.3	24.3	48%	159	100%	XM_017313447.1
PREDICTED: Mus musculus coiled-coil domain containing 33 (Ccdc33), transcript variant X4, mRNA	24.3	24.3	48%	159	100%	XM_017313446.1
PREDICTED: Mus musculus coiled-coil domain containing 33 (Ccdc33), transcript variant X3, mRNA	24.3	24.3	48%	159	100%	XM_017313445.1
PREDICTED: Mus musculus coiled-coil domain containing 33 (Ccdc33), transcript variant X2, mRNA	24.3	24.3	48%	159	100%	XM_017313444.1
PREDICTED: Mus musculus DIS3 like exosome 3'-5' exoribonuclease (Dis3l), transcript variant X3, mRNA	24.3	24.3	48%	159	100%	XM_006510982.3
PREDICTED: Mus musculus DIS3 like exosome 3'-5' exoribonuclease (Dis3l), transcript variant X2, mRNA	24.3	24.3	48%	159	100%	XM_006510983.3
PREDICTED: Mus musculus asparaginyl-tRNA synthetase 2 (mitochondrial)(putative) (Nars2), transcript variant X16, misc_RNA	24.3	24.3	48%	159	100%	XR_001785558.1
PREDICTED: Mus musculus asparaginyl-tRNA synthetase 2 (mitochondrial)(putative) (Nars2), transcript variant X15, misc_RNA	24.3	24.3	48%	159	100%	XR_001785557.1
PREDICTED: Mus musculus asparaginyl-tRNA synthetase 2 (mitochondrial)(putative) (Nars2), transcript variant X14, misc_RNA	24.3	24.3	48%	159	100%	XR_001785556.1
PREDICTED: Mus musculus asparaginyl-tRNA synthetase 2 (mitochondrial)(putative) (Nars2), transcript variant X13, misc_RNA	24.3	24.3	48%	159	100%	XR_001785555.1
Mus musculus FERM domain containing 4A (Frmd4a), transcript variant 4, mRNA	24.3	24.3	48%	159	100%	NM_001347086.1

Supplementary Table 4. Sequence alignment of Yy1-VMO.

description	maximal score	total score	query cover	E value	identity	accession
PREDICTED: Mus musculus aryl hydrocarbon receptor nuclear translocator (Arnt), transcript variant X5, misc_RNA	50.1	50.1	100%	3,00E-06	100%	XR_001783644.1
PREDICTED: Mus musculus aryl hydrocarbon receptor nuclear translocator (Arnt), transcript variant X4, misc_RNA	50.1	50.1	100%	3,00E-06	100%	XR_001783643.1
PREDICTED: Mus musculus aryl hydrocarbon receptor nuclear translocator (Arnt), transcript variant X2, mRNA	50.1	50.1	100%	3,00E-06	100%	XM_006500931.3
PREDICTED: Mus musculus aryl hydrocarbon receptor nuclear translocator (Arnt), transcript variant X1, mRNA	50.1	50.1	100%	3,00E-06	100%	XM_006500930.3
PREDICTED: Mus musculus aryl hydrocarbon receptor nuclear translocator (Arnt), transcript variant X6, mRNA	50.1	50.1	100%	3,00E-06	100%	XM_006500933.2
Mus musculus aryl hydrocarbon receptor nuclear translocator (Arnt), transcript variant 2, mRNA	50.1	50.1	100%	3,00E-06	100%	NM_009709.4
Mus musculus aryl hydrocarbon receptor nuclear translocator (Arnt), transcript variant 1, mRNA	50.1	50.1	100%	3,00E-06	100%	NM_001037737.2
PREDICTED: Mus musculus UDP-GlcNAc:betaGal beta-1,3-N-acetylglucosaminyltransferase 4 (B3gnt4), transcript variant X3, mRNA	30.2	30.2	60%	2.6	100%	XM_011248200.2
PREDICTED: Mus musculus UDP-GlcNAc:betaGal beta-1,3-N-acetylglucosaminyltransferase 4 (B3gnt4), transcript variant X1, mRNA	30.2	30.2	60%	2.6	100%	XM_011248199.2
PREDICTED: Mus musculus uncharacterized LOC666331 (LOC666331), transcript variant X1, mRNA	28.2	28.2	56%	10	100%	XM_006533962.2
PREDICTED: Mus musculus predicted gene, 35562 (Gm35562), transcript variant X11, ncRNA	28.2	28.2	56%	10	100%	XR_878497.1
PREDICTED: Mus musculus predicted gene, 35562 (Gm35562), transcript variant X10, ncRNA	28.2	28.2	56%	10	100%	XR_878495.1
Mus musculus uncharacterized LOC666331 (LOC666331), mRNA	28.2	28.2	56%	10	100%	NM_001256318.1
PREDICTED: Mus musculus predicted gene, 29862 (Gm29862), transcript variant X5, ncRNA	28.2	28.2	56%	10	100%	XR_872158.2
PREDICTED: Mus musculus predicted gene, 29862 (Gm29862), transcript variant X4, ncRNA	28.2	28.2	56%	10	100%	XR_872157.2
PREDICTED: Mus musculus predicted gene, 29862 (Gm29862), transcript variant X3, ncRNA	28.2	28.2	56%	10	100%	XR_380917.3
PREDICTED: Mus musculus predicted gene, 29862 (Gm29862), transcript variant X2, ncRNA	28.2	28.2	56%	10	100%	XR_001779668.1
PREDICTED: Mus musculus predicted gene, 29862 (Gm29862), transcript variant X1, ncRNA	28.2	28.2	56%	10	100%	XR_872156.2
PREDICTED: Mus musculus insulin-like growth factor I receptor (Igf1r), transcript variant X6, mRNA	26.3	26.3	52%	40	100%	XM_017321986.1
PREDICTED: Mus musculus insulin-like growth factor I receptor (Igf1r), transcript variant X5, mRNA	26.3	26.3	52%	40	100%	XM_006540645.3
PREDICTED: Mus musculus insulin-like growth factor I receptor (Igf1r), transcript variant X4, mRNA	26.3	26.3	52%	40	100%	XM_006540644.3
PREDICTED: Mus musculus insulin-like growth factor I receptor (Igf1r), transcript variant X3, mRNA	26.3	26.3	52%	40	100%	XM_006540643.3
PREDICTED: Mus musculus insulin-like growth factor I receptor (Igf1r), transcript variant X2, mRNA	26.3	26.3	52%	40	100%	XM_006540642.3
PREDICTED: Mus musculus insulin-like growth factor I receptor (Igf1r), transcript variant X1, mRNA	26.3	26.3	52%	40	100%	XM_006540641.3
PREDICTED: Mus musculus argininosuccinate lyase (Asl), transcript variant X2, mRNA	26.3	48.6	84%	40	100%	XM_017320601.1
PREDICTED: Mus musculus transmembrane protein 68 (Tmem68), transcript variant X4, misc_RNA	26.3	26.3	52%	40	100%	XR_390344.2
PREDICTED: Mus musculus transmembrane protein 68 (Tmem68), transcript variant X3, mRNA	26.3	26.3	52%	40	100%	XM_006538270.3
PREDICTED: Mus musculus transmembrane protein 68 (Tmem68), transcript variant X2, mRNA	26.3	26.3	52%	40	100%	XM_006538269.3
PREDICTED: Mus musculus transmembrane protein 68 (Tmem68), transcript variant X1, misc_RNA	26.3	26.3	52%	40	100%	XR_001784202.1
PREDICTED: Mus musculus neuregulin 2 (Nrg2), transcript variant X1, mRNA	26.3	26.3	52%	40	100%	XM_006525461.3
PREDICTED: Mus musculus transcription factor 20 (Tcf20), transcript variant X6, mRNA	26.3	26.3	52%	40	100%	XM_011245554.2
PREDICTED: Mus musculus transcription factor 20 (Tcf20), transcript variant X5, mRNA	26.3	26.3	52%	40	100%	XM_011245553.2
PREDICTED: Mus musculus transcription factor 20 (Tcf20), transcript variant X4, mRNA	26.3	26.3	52%	40	100%	XM_011245552.2
PREDICTED: Mus musculus transcription factor 20 (Tcf20), transcript variant X2, mRNA	26.3	26.3	52%	40	100%	XM_006520732.2
PREDICTED: Mus musculus transcription factor 20	26.3	26.3	52%	40	100%	XM_011245551.2

(Tcf20), transcript variant X1, mRNA						
PREDICTED: Mus musculus trans-acting transcription factor 8 (Sp8), transcript variant X8, mRNA	26.3	26.3	52%	40	100%	XM_006515988.3
PREDICTED: Mus musculus trans-acting transcription factor 8 (Sp8), transcript variant X7, mRNA	26.3	26.3	52%	40	100%	XM_006515987.3
PREDICTED: Mus musculus trans-acting transcription factor 8 (Sp8), transcript variant X6, mRNA	26.3	26.3	52%	40	100%	XM_006515986.3
PREDICTED: Mus musculus trans-acting transcription factor 8 (Sp8), transcript variant X5, mRNA	26.3	26.3	52%	40	100%	XM_006515985.3
PREDICTED: Mus musculus trans-acting transcription factor 8 (Sp8), transcript variant X4, mRNA	26.3	26.3	52%	40	100%	XM_006515984.3
PREDICTED: Mus musculus trans-acting transcription factor 8 (Sp8), transcript variant X3, mRNA	26.3	26.3	52%	40	100%	XM_011244124.2
PREDICTED: Mus musculus trans-acting transcription factor 8 (Sp8), transcript variant X2, mRNA	26.3	26.3	52%	40	100%	XM_006515983.3
PREDICTED: Mus musculus trans-acting transcription factor 8 (Sp8), transcript variant X1, mRNA	26.3	26.3	52%	40	100%	XM_006515982.3
PREDICTED: Mus musculus transcription factor 20 (Tcf20), transcript variant X3, mRNA	26.3	26.3	52%	40	100%	XM_006520733.1
PREDICTED: Mus musculus sodium channel, voltage-gated, type V, alpha (Scn5a), transcript variant X4, mRNA	26.3	26.3	52%	40	100%	XM_006511997.1
PREDICTED: Mus musculus sodium channel, voltage-gated, type V, alpha (Scn5a), transcript variant X3, mRNA	26.3	26.3	52%	40	100%	XM_006511996.1
PREDICTED: Mus musculus sodium channel, voltage-gated, type V, alpha (Scn5a), transcript variant X2, mRNA	26.3	26.3	52%	40	100%	XM_006511995.1
PREDICTED: Mus musculus sodium channel, voltage-gated, type V, alpha (Scn5a), transcript variant X1, mRNA	26.3	26.3	52%	40	100%	XM_006511993.1
Mus musculus sodium channel, voltage-gated, type V, alpha (Scn5a), transcript variant 2, mRNA	26.3	26.3	52%	40	100%	NM_001253860.1
Mus musculus sodium channel, voltage-gated, type V, alpha (Scn5a), transcript variant 1, mRNA	26.3	26.3	52%	40	100%	NM_021544.4
Mus musculus trans-acting transcription factor 8 (Sp8), mRNA	26.3	26.3	52%	40	100%	NM_177082.4
Mus musculus BCL2-associated athanogene 3 (Bag3), mRNA	26.3	26.3	52%	40	100%	NM_013863.5
Mus musculus transcription factor 20 (Tcf20), transcript variant 1, mRNA	26.3	26.3	52%	40	100%	NM_001114140.1
Mus musculus transcription factor 20 (Tcf20), transcript variant 2, mRNA	26.3	26.3	52%	40	100%	NM_013836.3
Mus musculus transmembrane protein 68 (Tmem68), mRNA	26.3	26.3	52%	40	100%	NM_028097.3
Mus musculus insulin-like growth factor I receptor (Igf1r), mRNA	26.3	26.3	52%	40	100%	NM_010513.2
Mus musculus receptor tyrosine kinase-like orphan receptor 2 (Ror2), mRNA	26.3	26.3	52%	40	100%	NM_013846.3
Mus musculus tRNA methyltransferase O (Trmo), transcript variant 2, mRNA	24.3	24.3	48%	159	100%	NM_001347095.1
Mus musculus transforming growth factor, beta 2 (Tgfb2), transcript variant 1, mRNA	24.3	24.3	48%	159	100%	NM_009367.4
Mus musculus transforming growth factor, beta 2 (Tgfb2), transcript variant 2, mRNA	24.3	24.3	48%	159	100%	NM_001329107.1
PREDICTED: Mus musculus predicted gene, 33746 (Gm33746), transcript variant X3, ncRNA	24.3	24.3	48%	159	100%	XR_001778574.1
PREDICTED: Mus musculus predicted gene, 33746 (Gm33746), transcript variant X2, ncRNA	24.3	24.3	48%	159	100%	XR_379069.3
PREDICTED: Mus musculus predicted gene, 33746 (Gm33746), transcript variant X1, ncRNA	24.3	24.3	48%	159	100%	XR_001778573.1
PREDICTED: Mus musculus cytosolic thiouridylase subunit 2 (Ctu2), transcript variant X3, mRNA	24.3	24.3	48%	159	100%	XM_011248490.2
PREDICTED: Mus musculus cytosolic thiouridylase subunit 2 (Ctu2), transcript variant X2, mRNA	24.3	24.3	48%	159	100%	XM_011248489.2
PREDICTED: Mus musculus cytosolic thiouridylase subunit 2 (Ctu2), transcript variant X1, misc_RNA	24.3	24.3	48%	159	100%	XR_878872.2
PREDICTED: Mus musculus nuclear factor of activated T cells 5 (Nfat5), transcript variant X3, mRNA	24.3	24.3	48%	159	100%	XM_006531193.3
PREDICTED: Mus musculus nuclear factor of activated T cells 5 (Nfat5), transcript variant X2, mRNA	24.3	24.3	48%	159	100%	XM_006531192.3
PREDICTED: Mus musculus nuclear factor of activated T cells 5 (Nfat5), transcript variant X1, mRNA	24.3	24.3	48%	159	100%	XM_006531191.3
PREDICTED: Mus musculus glycerol-3-phosphate acyltransferase 4 (Gpat4), transcript variant X1, mRNA	24.3	24.3	48%	159	100%	XM_011242104.2
PREDICTED: Mus musculus predicted gene, 39079 (Gm39079), ncRNA	24.3	24.3	48%	159	100%	XR_869909.2
PREDICTED: Mus musculus RIKEN cDNA 9430038I01	24.3	24.3	48%	159	100%	XM_006508331.3

gene (9430038I01Rik), transcript variant X4, mRNA						
PREDICTED: Mus musculus RIKEN cDNA 9430038I01 gene (9430038I01Rik), transcript variant X3, mRNA	24.3	24.3	48%	159	100%	XM_006508329.3
PREDICTED: Mus musculus RIKEN cDNA 9430038I01 gene (9430038I01Rik), transcript variant X2, mRNA	24.3	24.3	48%	159	100%	XM_011241949.2
PREDICTED: Mus musculus RIKEN cDNA 9430038I01 gene (9430038I01Rik), transcript variant X1, mRNA	24.3	24.3	48%	159	100%	XM_011241948.2
PREDICTED: Mus musculus signal-induced proliferation-associated 1 like 3 (Sipa1l3), transcript variant X15, mRNA	24.3	24.3	48%	159	100%	XM_006540405.2
PREDICTED: Mus musculus signal-induced proliferation-associated 1 like 3 (Sipa1l3), transcript variant X14, mRNA	24.3	24.3	48%	159	100%	XM_011250732.2
PREDICTED: Mus musculus signal-induced proliferation-associated 1 like 3 (Sipa1l3), transcript variant X13, mRNA	24.3	24.3	48%	159	100%	XM_006540404.3
PREDICTED: Mus musculus signal-induced proliferation-associated 1 like 3 (Sipa1l3), transcript variant X11, mRNA	24.3	24.3	48%	159	100%	XM_006540402.3
PREDICTED: Mus musculus signal-induced proliferation-associated 1 like 3 (Sipa1l3), transcript variant X10, mRNA	24.3	24.3	48%	159	100%	XM_006540401.3
PREDICTED: Mus musculus signal-induced proliferation-associated 1 like 3 (Sipa1l3), transcript variant X9, mRNA	24.3	24.3	48%	159	100%	XM_006540400.3
PREDICTED: Mus musculus signal-induced proliferation-associated 1 like 3 (Sipa1l3), transcript variant X8, mRNA	24.3	24.3	48%	159	100%	XM_006540399.3
PREDICTED: Mus musculus signal-induced proliferation-associated 1 like 3 (Sipa1l3), transcript variant X7, mRNA	24.3	24.3	48%	159	100%	XM_011250731.2
PREDICTED: Mus musculus signal-induced proliferation-associated 1 like 3 (Sipa1l3), transcript variant X6, mRNA	24.3	24.3	48%	159	100%	XM_011250730.2
PREDICTED: Mus musculus signal-induced proliferation-associated 1 like 3 (Sipa1l3), transcript variant X5, mRNA	24.3	24.3	48%	159	100%	XM_011250729.2
PREDICTED: Mus musculus signal-induced proliferation-associated 1 like 3 (Sipa1l3), transcript variant X4, mRNA	24.3	24.3	48%	159	100%	XM_011250728.2
PREDICTED: Mus musculus signal-induced proliferation-associated 1 like 3 (Sipa1l3), transcript variant X3, mRNA	24.3	24.3	48%	159	100%	XM_006540397.3
PREDICTED: Mus musculus signal-induced proliferation-associated 1 like 3 (Sipa1l3), transcript variant X2, mRNA	24.3	24.3	48%	159	100%	XM_017312346.1
PREDICTED: Mus musculus signal-induced proliferation-associated 1 like 3 (Sipa1l3), transcript variant X1, mRNA	24.3	24.3	48%	159	100%	XM_011250727.2
PREDICTED: Mus musculus acid phosphatase, testicular (Acpt), transcript variant X5, mRNA	24.3	24.3	48%	159	100%	XM_011250772.2
PREDICTED: Mus musculus acid phosphatase, testicular (Acpt), transcript variant X4, mRNA	24.3	24.3	48%	159	100%	XM_017321902.1
PREDICTED: Mus musculus acid phosphatase, testicular (Acpt), transcript variant X3, mRNA	24.3	24.3	48%	159	100%	XM_017321901.1
PREDICTED: Mus musculus acid phosphatase, testicular (Acpt), transcript variant X2, mRNA	24.3	24.3	48%	159	100%	XM_006540531.3
PREDICTED: Mus musculus acid phosphatase, testicular (Acpt), transcript variant X1, mRNA	24.3	24.3	48%	159	100%	XM_006540530.3
PREDICTED: Mus musculus tRNA methyltransferase O (Trmo), transcript variant X4, mRNA	24.3	24.3	48%	159	100%	XM_017320423.1
PREDICTED: Mus musculus tRNA methyltransferase O (Trmo), transcript variant X1, mRNA	24.3	24.3	48%	159	100%	XM_017320422.1
PREDICTED: Mus musculus RIKEN cDNA 1700024P16 gene (1700024P16Rik), transcript variant X1, mRNA	24.3	24.3	48%	159	100%	XM_017320219.1
PREDICTED: Mus musculus glial cell line derived neurotrophic factor family receptor alpha 4 (Gfra4), transcript variant X3, misc_RNA	24.3	24.3	48%	159	100%	XR_001780826.1
PREDICTED: Mus musculus neuropilin (NRP) and tolloid (TLL)-like 1 (Neto1), transcript variant X12, mRNA	24.3	24.3	48%	159	100%	XM_011247081.2
Mus musculus N-acetylglucosamine-1-phosphotransferase, gamma subunit (Gnptg), transcript variant 2, mRNA	24.3	24.3	48%	159	100%	NM_001346737.1

Supplementary Table 5. Sequence alignment of Arnt-VMO.

ID#	disease
S3060	diabetic nephropathy
S3170	hypertensive nephrosclerosis
S3584	FSGS
P11150/17	autoimmune hepatitis
P9446/17	liver fibrosis
P14203/17	liver cirrhosis
7183/17	lung fibrosis

Supplementary Table 6. Human disease specimens.

ID#	% fibrosis	pre-medication	disease	creatinine [mg/dL]	BUN [mg/dL]	eGFR [mL/min]
S3752	25-30	CsA	FSGS	3.3	56	25
S3564	20	FK506	nephrosclerosis	3.2	74	16
S3896	15-20	FK506	ADPKD	3.0	97	23

Supplementary Table 7. Kidney transplant patient characteristics.

system	comparison	*slope*	r^2	*p* value
renal cortex	*ARNT* vs. *FKBP12* *ARNT* vs. *YY1*	*-2.6±0.4* *-0.6±0.0*	*0.9618* *0.9922*	*0.0193* *0.0039*
cardiovascular	*ARNT* vs. *FKBP12* *ARNT* vs. *YY1*	*-1.8±0.8* *-1.1±0.5*	*0.2843* *0.3012*	*0.0606* *0.0521*
digestive	*ARNT* vs. *FKBP12* *ARNT* vs. *YY1*	*-1.2±0.5* *-0.7±0.3*	*0.1439* *0.1152*	*0.0093* *0.0210*
central nervous	*ARNT* vs. *FKBP12* *ARNT* vs. *YY1*	*-0.9±0.3* *-1.1±0.2*	*0.0590* *0.2368*	*0.0015* *<0.0001*
lymphatic	*ARNT* vs. *FKBP12* *ARNT* vs. *YY1*	*-0.9±0.7* *-0.7±0.8*	*0.1129* *0.0503*	*0.2032* *0.4037*
reproductive	*ARNT* vs. *FKBP12* *ARNT* vs. *YY1*	*-0.6±0.5* *-0.7±0.4*	*0.0345* *0.1119*	*0.2931* *0.0531*
endocrine	*ARNT* vs. *FKBP12* *ARNT* vs. *YY1*	*-0.6±0.7* *-2.0±0.6*	*0.0290* *0.2917*	*0.4055* *0.0044*
peripheral nervous	*ARNT* vs. *FKBP12* *ARNT* vs. *YY1*	*-0.4±0.7* *-0.5±0.3*	*0.0169* *0.0911*	*0.5447* *0.1517*
respiratory	*ARNT* vs. *FKBP12* *ARNT* vs. *YY1*	*1.7±1.4* *0.6±0.4*	*0.1708* *0.2667*	*0.2689* *0.1546*

Supplementary Table 8. In publicly available datasets (accession number GSE3526), expression levels of *ARNT* inversely correlated with *FKBP12* and *YY1* expression levels is not limited to the kidney (renal cortex), but also evident in cardiovascular, digestive and central nervous systems (slope, r^2 and values of *p* were calculated by linear regression).

VMO	sequence	supplier
control-VMO	5'-CCTCTTACCTCAGTTACAATTTATA-3'	Gene Tools, Philomath, USA (1)
Arnt-VMO	5'-AAGAGCCACTCCGCAGATTAGGCAC-3'	Gene Tools, Philomath, USA (1)
Fkbp12-VMO	5'-AGATGGTCTCCACCTGCACTCCCAT-3'	Gene Tools, Philomath, USA (1)
Yy1-VMO	5'-TGTAGAGGGTGTCGCCCGAGGCCAT-3'	Gene Tools, Philomath, USA (1)

Supplementary Table 9. In vivo-morpholino sequences.

gene	**forward primer sequence** **reverse primer sequence**	**supplier**
Acta2 (mouse)	5'-CTCTTCCAGCCATCTTTCATTG-3' 5'-GTTGTTAGCATAGAGATCCTTCCT-3'	PrimerDesign, Southampton, UK
Actb (mouse)	undisclosed undisclosed	PrimerDesign, Southampton, UK
Ahr (mouse)	5'-GCCCTTCCCGCAAGATGTTAT-3' 5'-TCAGCAGGGGTGGACTTTAAT-3'	Eurofins MWG Operon (2)
Alk3 (mouse)	5'-TGTCATTCTAGCCATGTTTTACC-3' 5'-ACCAAGGATCAGATGTGAGAC-3'	PrimerDesign, Southampton, UK
ALK3 (human)	5'- GGACATTGCTTTGCCATCATAG-3' 5'- GGGCTTTTGGAGAATCTTTGC-3'	PrimerDesign, Southampton, UK
Alk5 (mouse)	5'-TCTGCATTGCACTTATGCTGA-3' 5'-AAAGGGCGATCTAGTGATGGA-3'	Eurofins MWG Operon (2)
Alk6 (mouse)	5'-GCGGCCTATGCCATTTACAC -3' 5'-AGTCTCGATGGGCGATTGC-3'	Eurofins MWG Operon (3)
Ar (mouse)	5'-AAGAGCCGCTGAAGGGAAA-3' 5'-GAGACGACAAGATGGGCAAAT-3'	PrimerDesign, Southampton, UK
Arnt (mouse)	5'-CCTTCAGTGCTATGTCTCTTCC-3' 5'-CAGTCTCAGGAGGAAAGTTGGA-3'	PrimerDesign, Southampton, UK
ARNT (human)	5'- AGAGAGACTTGCCAGGGAAAAT-3' 5'- AGTTCTGTGATGTAGGCTGTCA-3'	PrimerDesign, Southampton, UK
Cebpb (mouse)	5'-ACGGGACTGACGCAACAC-3' 5'-AACAAAAACAAAACCAAAAAACATCAAC-3'	PrimerDesign, Southampton, UK
Col1a1 (mouse)	5'-ATGGATTCCCGTTCGAGTACG-3' 5'-TCAGCTGGATAGCGACATCG-3'	Eurofins MWG Operon (4, 5)
Creb1 (mouse)	5'-TTGAGTAAGGCTGAGCATGATC-3' 5'-TCTTAACTTTAAACTGCGGAACAC-3'	PrimerDesign, Southampton, UK
Fkbp12 (mouse)	5'-CTATGCCTATGGAGCCACCG-3' 5'-ATCCACGTGCAGAGCTAAGG-3'	Eurofins MWG Operon (6)
FKBP12 (human)	5'-GTGGAAACCATCTCCCCAGG-3' 5'-CCATCTTCAAGCATCCCGGT-3'	Eurofins MWG Operon (6)
Fkbp25 (mouse)	5'-TTCTGCAGGATCACGGTTCA-3' 5'-TGGTCCTTATTAGCAGTCTTGGC-3'	Eurofins MWG Operon (6)
Fkbp38 (mouse)	5'-GCTGGGAGACTGCGATGTTA-3' 5'-GTATGGGCTCCTGCTGCC-3'	Eurofins MWG Operon (6)
Fkbp52 (mouse)	5'-ACCGCGTACTTCAAGGAAGG-3' 5'-ACCGGAGAAGCTAGACTCGT-3'	Eurofins MWG Operon (6)
Gapdh (mouse)	undisclosed undisclosed	PrimerDesign, Southampton, UK
GAPDH (human)	undisclosed undisclosed	PrimerDesign, Southampton, UK
Gata3 (mouse)	5'-GAAGACTTTATTGTACCTGGATAGC-3' 5'-TGGACATCAGACTTAGTGGTTTC-3'	PrimerDesign, Southampton, UK
Hif1α (mouse)	5'-TCACCAGACAGAGCAGGAAA-3' 5'-GCGAAGCTATTGTCTTTGGG-3'	Eurofins MWG Operon (7)
Max (mouse)	5'-GTGAGTGAGTGAGCGAGTGA-3' 5'-GGAGGGGTGGAGGGAAGG-3'	PrimerDesign, Southampton, UK
Yy1 (mouse)	5'-GCCCTTTCAGTGCACATTCG-3' 5'-CTCCGGTATGGATTCGCACA-3'	Eurofins MWG Operon (6)
YY1 (human)	5'-AACAGGCATCCCGAGTTCAG-3' 5'-GCGGTGGTACAGATGCTTCA-3'	Eurofins MWG Operon (6)

Supplementary Table 10. Oligonucleotide sequences for qRT-PCR.

gene	**forward primer sequence** **reverse primer sequence**	**supplier**
Arnt motif (mouse)	5'-GACTTCAGTTCAGCCGGCTCTC-3' 5'-CTCTGGTTCTGGCCCGCCGGGAGG-3'	Eurofins MWG Operon

Supplementary Table 11. Oligonucleotide sequences for ChIP.

Supplemental Experimental Procedures

FK506/CsA preparation and treatment. FK506 and Cyclosporine A (CsA) were purchased as powders with a purity of >98% (Abcam Biochemicals, Cambridge, UK). FK-506 and CsA stock solutions (0.2 mg/mL) were prepared by dissolving the compound in saline (0.9% NaCl) containing 1.25% PEG40 Castor Oil (spectrum chemicals & laboratory products, USA) and 2% ethanol. On the basis of an average drinking volume of 3 mL and a body weight of 20 g per mouse, FK506 and CsA stock solutions were diluted in glucose-water (5%) and orally applied. One day before surgery, mice were treated orally with either vehicle buffer glucose (5%), with 0.02, 0.075, 0.2, 5.0 mg/kg body weight per day FK506, or 10 mg/kg body weight per day CsA, respectively. Solutions were changed once a day and mice were sacrificed at indicated time points.

FK506 blood concentration measurements. FK506 concentration in whole blood samples of mice was measured using colorimetric FK506 Elisa Kit (Abnova, Taipei, Japan) according to the manufacturer's protocol. Briefly, 25 µL of whole blood samples and standard solutions containing 0, 2, 10 and 50 ng/mL FK506 were analyzed by OD measurements at 450 nanometer (nm) wavelength.

LDN-193189 treatment. Mice were injected intraperitoneally with 3 mg/kg body weight per day LDN-193189 (LDN, Sigma, St. Louis, USA) in DMSO twice daily starting one day prior of surgery, control mice received equivalent volume of vehicle DMSO.

In vivo-morpholino (VMO) treatment. Mice were injected intraperitoneally with 12.5 mg/kg body weight in vivo-morpholinos (Gene Tools, Philomath, USA) in saline at a final volume of 100 µL every other day starting two days prior of surgery (1), sequence alignments were performed using NCBI Nucleotide Blast and are listed in **Supplementary Tables 3-5** (9). A control in vivo-morpholino that targets a human β-globin intron mutation was used as standard control (10). In vivo-morpholino sequences are listed in **Supplemental Table 9**.

GPI-1046 treatment. Mice were injected subcutaneously with 10 mg/kg body weight per day GPI-1046 (Santa Cruz Biotechnology, Dallas, USA) in DMSO once daily starting one day prior of surgery, control mice received equivalent volume of vehicle DMSO. For oral administration, GPI-1046 stock solution was diluted in glucose-water (5%) and orally applied on the basis of an average drinking volume of 3

mL and a body weight of 20 g per mouse. Three days after challenging with UUO, mice were treated orally with either vehicle buffer glucose (5%) or 30 mg/kg body weight per day GPI-1046, respectively.

Histology. Paraffin-embedded specimens were sectioned at 3 µm, periodic acid–Schiff (PAS), Masson's Trichrome Stain (MTS) and Sirius Red/Fast green was performed at the University Medicine Göttingen. For morphometric analysis of interstitial fibrosis, fibrotic areas were assessed by using cellSens (Olympus, Tokyo, Japan) software. Ten visual fields were selected randomly for each MTS stained section at 200x magnification and the relative interstitial fibrotic area was evaluated by using a 10 mm^2 graticule. Tubular damage was analysed after PAS stain and graded according to a semi-quantitative score of 0 to 3 (0: normal, 1: mild, 2: moderate, 3: severe) at 400x magnification in a total number of 100 tubules per section (4). To evaluate collagen deposition, sections were stained with Sirius red in a saturated aqueous solution of picric acid containing 0.1% Direct Red 80 (Sigma, St. Louis, USA), ten visual fields were selected randomly for each section at 400x magnification and evaluated by using a 10 mm^2 graticule.

Immunohistochemistry. Paraffin-embedded specimens were deparaffinized in xylene and rehydrated in ethanol containing distilled water. Tissue sections were stained using polyclonal antibodies against ALK3 (sc-20736, Santa Cruz Biotechnology, Dallas, USA) and ARNT (3718S, Cell Signaling, Danvers, USA), peroxidase labeling was performed using Vectastain Universal Elite ABC Kit (Vector Laboratories, Burlingame, USA) according to the manufacturer's protocol. AEC Substrate-Chromogen (Dako, Glostrup, Denmark) was applied for peroxidase visualization according to the manufacturer's protocol. Nuclear counterstain was performed by using Mayer's Hematoxylin Solution (Sigma, St. Louis, USA).

Immunofluorescence. For immunofluorescent staining, primary antibodies against ARNT (5537S, Cell Signaling, Danvers, USA), Hif1α (H6535, Sigma, St. Louis, USA), Hif2α (ab20654, Abcam Biochemicals, Cambridge, UK), phosphorylated Smad1/5/8 (pSmad1/5/8, sc-12353, Santa Cruz Biotechnology, Dallas, USA), CD45 (550539, BD Biosciences, Franklin Lakes, USA), Collagen-1 (ab34710, Abcam Biochemicals, Cambridge, UK), α-smooth muscle actin (αSMA, A5228, Sigma, St. Louis, USA), FKBP12 (ab2918, Abcam Biochemicals, Cambridge, UK) and YY1 (ab12132, Abcam Biochemicals, Cambridge, UK) were used, secondary antibodies were labeled with Alexa Fluor 488 or

568 (Life Technologies, Carlsbad, USA). Renal basement membranes were stained with antibodies against Collagen-4 (1340-30, SouthernBiotech, Birmingham, USA), cardiac cell membranes with antibodies against WGA (W11261, Life Technologies, Carlsbad, USA). Nuclear staining was performed using 4',6-diamidino-2-phenylindole (DAPI, Vector Laboratories, Burlingame, USA). Relative areas positive for Collagen-1, αSMA, tubular nuclei positive for ARNT and pSmad1/5/8 were quantified in 10 high power fields per section at 400x magnification, representative confocal pictures are shown.

In vitro stimulation. For RNA extractions, cells were seeded in 6 well culture plates at 10^5 cells per well in antibiotic free standard growth medium. After 24 hours, cells were stimulated with FK506 (Abcam Biochemicals, Cambridge, UK) or Cyclosporin A (CsA, Sigma, St. Louis, USA) dissolved in DMSO at indicated concencentrations. Cells were harvested for further analysis 6 hours after incubation. To examine *de novo* protein syntheses, cells were again plated in 6 well culture plates as initially described and then pre-treated with the translation blocker Cycloheximide (CHX, 10 µg/mL, Sigma, St. Louis, USA). After one hour of incubation, 200 pM FK506 was applied for additional 6 hours.

In vitro transfection. One night before transfection, MCT cells were seeded in 6 well culture plates at a concentration of 1.5-2 x 10^5 per well in antibiotic-free DMEM (Gibco, Carlsbad, USA) supplemented with 10% heat-inactivated fetal bovine serum (FBS, Sigma, St. Louis, USA). For knockdown experiments, 60 pmol siRNA (Santa Cruz Biotechnology, Dallas, USA) or scrambled siRNA (scrRNA, Santa Cruz Biotechnology, Santa Cruz, USA) was transfected, for over-expression experiments, 2 µg plasmid DNA was transfected using Lipofectamine 2000 reagent (Invitrogen, Carlsbad, USA). After 4 hours of incubation, transfection medium was replaced by antibiotic-free medium and cells recovered overnight. For stimulation experiments, cells were stimulated the day after with 200 pM FK506 (Abcam Biochemicals, Cambridge, UK) dissolved in DMSO and harvested after 6 hours of incubation for RNA and protein analysis.

***Alk3* promoter constructs.** Site-directed mutagenesis of the palindromic E-box motif *CACGTG* to *TATATA* within the proximal *ALK3* promoter was performed using a QuikChange XL Site-Directed Mutagenesis Kit (Agilent Technologies, Santa Clara, USA). The original *ALK3* promoter construct (Gene Universal Inc., Newark, USA) was fragmented into two parts (335 and 794 bp) using PCR amplification and restriction digestion. The 335 bp fragment containing the E-box binding site was

amplified using primers with KpnI (primer sequence: 5'-GGGGGTACCGAGGTAGTGACAGTTCTT-3') and BsmI cutting sites (primer sequence: 5'-CCCTGCATTCATTACTCA-3'). The purified PCR products were cloned into *pGEM-T-Easy* (Promega, Madison, USA) vector for site-directed mutagenesis (primer sequence: 5'-GTGATCCGGAGAACGCTATATACTCCACGTTCCTCCCG-3' and 5'-GTAGCGAAAGCCTGGTTTCG-3'). The reaction was carried out according to the manufacturer's recommendation containing 10 ng of DNA template, 5 µL of 10x reaction buffer, 125 ng of primers, 1 µL of dNTP mix, 3 µl of QuikSolution and 1 µL of PfuTurbo DNA polymerase in a final volume of 50 µL. The thermal cycling condition was initiated with a denaturating step at 95°C for 3 minutes followed by 25 cycles containing 95°C for 50 seconds, 60°C for 50 seconds, 68°C for 4 minuntes and a final extension at 68°C for 7 minuntes. 1 µL Dpn1 (2.5 U/µL) was added and incubated for 2 hours at 37°C to remove the original template from the reaction. The PCR reaction was transformed into XL10-Gold Ultracompetent Cells (Agilent Technologies, Santa Clara, USA). The resulting 335 bp mutated fragment was digested with KpnI/BsmI restriction enzymes and subcloned to a *pGL3-basic* vector (Promega, Madison, USA) together with the BsmI/HindIII digested 794 bp fragment. All plasmids were carefully sequenced to confirm that mutations were placed at the proper position.

Promoter Analysis. For promoter analysis, cells were co-transfected at 75% confluence with 4 µg plasmid DNA, 4 µg of promoter construct DNA and 0.1 µg renilla luciferase internal control vector *pGL4.73* (Promega, Madison, USA) in 6-well plates using Lipofectamine 2000 reagent (Invitrogen, Carlsbad, USA) according to the manufacturer´s instructions. Growth medium was not replaced during incubation. After 48 hours, transfected cells were washed in PBS. Firefly and renilla luciferase activity of 20 µL cell extract was determined using the Dual-Luciferase Reporter Assay System (Promega, Madison, USA) according to the manufacturer´s instructions. Signals were normalized to renilla luciferase for each sample.

RNA isolation. Total RNA was extracted from cells using TRIzol Reagent (Life technologies, Carlsbad, USA), tissue was shredded using TissueLyser LT (Qiagen, Hilden, Germany). Subsequent RNA purification procedure was performed by PureLink RNA Mini Kit (Ambion, Carlsbad, USA) according to the manufacturer's protocol.

Quantitative real-time PCR quantification (qRT-PCR). For SYBR-based real-time PCR, cDNA synthesis was performed by using DNase I digestion (Invitrogen, Carlsbad, USA) and SuperScript II Reverse Transcriptase (Invitrogen, Carlsbad, USA) according to the manufacturer's protocol. 1 µL of reverse-transcribed cDNA was added to the reaction mixture containing the primer pair (200 nmol/L each) and diluted 2x Fast SYBR Green Master Mix (Applied Biosystems, Carlsbad, USA) in a final volume of 20 µL for each PCR reaction. The real-time PCR reactions were performed in a 96-well reaction plate using the StepOne Plus Real-Time System (Applied Biosystems, Carlsbad, USA) and were done in triplicates. An initiation step at 95°C for 20 seconds was followed by 40 cycles at 95°C for 3 seconds and 60°C for 30 seconds, with one cycle of dissociation at 95°C for 15 seconds, 60°C for 60 seconds, and 95°C for 15 seconds. The intercalation of SYBR Green dye and its fluorescent signal is directly proportional to the amount of amplified DNA and was transformed into the cycle threshold (Ct). For normalization, the Ct values of the housekeeping genes *Gapdh* and *Actb* were subtracted from the Ct values of the gene of interest to generate the dCt values. The relative expression levels were calculated using the equation 2^{-ddCt}. Oligonucleotide sequences are listed in **Supplemental Table 10**.

RT^2 Profile PCR Array. To compare qPCR-validated cDNA samples after FK506 treatment and DMSO control, gene expression profiling was performed using commercially available plates (PAHS-075Z/PAMM-002Z/PAMM032Z, SABiosciences, Qiagen, Hilden, Germany). HK-2 cells were plated in 6 well culture plates as previously described and stimulated with 150 ng/mL FK506, MCT cells with 200 pM FK506. After 6 hours, cells were dissolved and RNA was isolated, digested and reverse transcripted. The 25 ng cDNA equivalent of total RNA was added to the reaction mixture containing diluted 2x RT² SYBR Green ROX qPCR Mastermix (Qiagen, Hilden, Germany) in a final volume of 25 µL for each well of the RT2 Profiler PCR. PCR reactions were performed under recommended thermal cycling conditions (10 min at 95°C, 15 s at 95°C, 1 min at 60°C for 40 cycles). To verify PCR specificity, dissociation curve analysis was generated. Relative levels of mRNA expression were normalized in all the samples with expression levels of included housekeeping genes, and data analysis was done using an web-based analysis software provided by SABiosciences. Transcription factor binding sites within the *ALK3* proximal promoter was performed 5000 basepairs relative to transcriptional start site using TRANSFAC database (11).

Western blot analyses. Tissue and cells were homogenized in NP40 lysis buffer (Life technologies, Carlsbad, USA) supplemented with protease inhibitor cocktail (Roche, Basel, Switzerland). After sonication, protein samples were resolved by a 4-12% Bis-Tris polyacrylamide gel electrophoresis system (Novex, Carlsbad, USA) and transferred onto a nitrocellulose membrane (GE Healthcare, Freiburg, Deutschland), followed by a blocking step with 5% dry milk or 5% bovine serum albumin (BSA) in TBS-T (TBS pH 7.2, 0.1% Tween-20) to prevent unspecific bindings. After incubation with respective primary antibodies against ALK3 (ABD51, Merck Millipore, Billerica, USA) and ALK6 (ABD50, Merck Millipore, Billerica, USA), pSmad1/5/8 (13820, Cell Signaling, Danvers, USA), Arnt (3718, Cell Signaling, Danvers, USA), Fkbp12 (ab2918, Abcam Biochemicals, Cambridge, UK), NFATc1 (sc-7294, Santa Cruz Biotechnology, Dallas, USA), NFATc2 (sc-7295, Santa Cruz Biotechnology, Dallas, USA), β-actin (A5316, Sigma, St. Louis, USA) and Gapdh (5G4, HyTest, Turku, Finland), secondary HRP-conjugated antibodies were used (Dako, Glostrup, Denmark). Luminescence was detected by using chemiluminescent substrate (Cell Signaling, Danvers, USA) on a ChemiDoc XRS system (Bio-Rad, Hercules, USA). Native protein samples were prepared with Native PAGE Sample Prep kit (Novex, Carlsbad, USA) according to the manufacturer's instruction. Non-denaturating native gel electrophoresis was performed with Native PAGE 3-12% Bis-Tris Protein gel (Novex, Carlsbad, USA).

Co-immunoprecipitation (CoIP). CoIP was performed with Protein G Immunoprecipitation Kit (Roche, Basel, Switzerland). Protein A/G PLUS Agarose beads (Santa Cruz Biotechnology, Santa Cruz, USA) were used for the lysate pre-cleaning and pull-down. For each CoIP, 2 x 10^7 MCT cells have been used following the manufacturer's instructions. Yy1 (ab12132, Abcam Biochemicals, Cambridge, UK), Fkbp12 (ab2918, Abcam Biochemicals, Cambridge, UK), Arnt (3718, Cell Signaling, Danvers, USA), GFP (MA5-15256, Thermo Fisher Scientific, Waltham, USA) and myc-tag antibodies (2276, Cell Signaling, Danvers, USA) were used for immunoprecipitation, detection of co-immunoprecipitated Fkbp12 (ab12132, Abcam Biochemicals, Cambridge, UK), Hif1α (H6535, Sigma, St. Louis, USA), Ahr (MA1-514, Thermo Fisher Scientific, Waltham, USA), GFP (MA5-15256, Thermo Fisher Scientific, Waltham, USA) and myc-tag (2276, Cell Signaling, Danvers, USA) was performed by immunoblotting.

Chromatin immunoprecipitation (ChIP). DNA and protein interaction was performed with the OneDay ChIP Kit (Diagenode, Seraing, Belgium) according to the manufacturer's instructions. 2 x 10^7 MCT cells have been used for each ChIP reaction. Cell lysates were sonicated using an ultrasonic processor S-4000 (Misonix, Farmingdale, USA). Immunoprecipitation was performed with a ChIP grade antibody against Yy1 (ab12132, Abcam Biochemicals, Cambridge, UK) and Arnt (3718, Cell Signaling, Danvers, USA). Enriched DNA was analyzed by qRT-PCR with EpiTect ChIP qPCR primers for genomic *Arnt* (Qiagen, Hilden, Germany), oligonucleotide sequences for genomic *Alk3* are listed in **Supplemental Table 11**.

Analyses of publicly available array datasets. Datasets provided publicly were analyzed according to general recommendations (12). For gene ontology analysis, 5% of most significant up-regulated genes in response to FK506 were extracted from Nephroseq database (nephroseq.org) based on genome-wide transcriptional expression datasets for bioactive small molecules (accession number GSE5258) (13, 14), and process analysis was performed using Gene Ontology enRIchment anaLysis and visuaLizAtion tool (GORILLA) using a value of $p<0.001$ threshold (15, 16). Protein-protein interactions were extracted from Search Tool for the Retrieval of Interacting Genes/Proteins (STRING) using highest confidence (score 0.900) (17), prediction of transcription factors regulating 5% of most significant up-regulated genes in response to FK506 extracted from Nephroseq database based on genome-wide transcriptional expression datasets for bioactive small molecules (accession number GSE5258) was performed using Predicting ASsociated Transcription factors from Annotated Affinities (PASTAA) within 200 basepairs upstream transcriptional start site, maximum affinity level and values of $p<0.05$ (13, 14, 18). Human transcriptome array data are shown as $\log_2$ median centered intensities extracted from Nephroseq database (accession numbers GSE69438, GSE66494, GSE35487, GSE30566, GSE21785, GSE1563, GSE3526) (19-25), and $\log_2$ expression values extracted from GEO2R (accession numbers GSE48944 and GSE14964) (26, 27).

Supplemental References

1. Morcos PA, Li Y, and Jiang S. Vivo-Morpholinos: a non-peptide transporter delivers Morpholinos into a wide array of mouse tissues. *Biotechniques.* 2008;45(6):613-4, 6, 8 passim.
2. Spandidos A, Wang X, Wang H, and Seed B. PrimerBank: a resource of human and mouse PCR primer pairs for gene expression detection and quantification. *Nucleic Acids Res.* 2010;38(Database issue):D792-9.
3. Sugimoto H, LeBleu VS, Bosukonda D, Keck P, Taduri G, Bechtel W, Okada H, Carlson W, Jr., Bey P, Rusckowski M, et al. Activin-like kinase 3 is important for kidney regeneration and reversal of fibrosis. *Nat Med.* 2012;18(3):396-404.
4. Bechtel W, McGoohan S, Zeisberg EM, Muller GA, Kalbacher H, Salant DJ, Muller CA, Kalluri R, and Zeisberg M. Methylation determines fibroblast activation and fibrogenesis in the kidney. *Nat Med.* 2010;16(5):544-50.
5. Tampe B, Tampe D, Zeisberg EM, Muller GA, Bechtel-Walz W, Koziolek M, Kalluri R, and Zeisberg M. Induction of Tet3-dependent Epigenetic Remodeling by Low-dose Hydralazine Attenuates Progression of Chronic Kidney Disease. *EBioMedicine.* 2015;2(1):19-36.
6. Ye J, Coulouris G, Zaretskaya I, Cutcutache I, Rozen S, and Madden TL. Primer-BLAST: a tool to design target-specific primers for polymerase chain reaction. *BMC Bioinformatics.* 2012;13(134.
7. Forristal CE, Brown AL, Helwani FM, Winkler IG, Nowlan B, Barbier V, Powell RJ, Engler GA, Diakiw SM, Zannettino AC, et al. Hypoxia inducible factor (HIF)-2alpha accelerates disease progression in mouse models of leukemia and lymphoma but is not a poor prognosis factor in human AML. *Leukemia.* 2015;29(10):2075-85.
8. Zhao X, Ho D, Gao S, Hong C, Vatner DE, and Vatner SF. Arterial Pressure Monitoring in Mice. *Curr Protoc Mouse Biol.* 2011;1(105-22.
9. Altschul SF, Madden TL, Schaffer AA, Zhang J, Zhang Z, Miller W, and Lipman DJ. Gapped BLAST and PSI-BLAST: a new generation of protein database search programs. *Nucleic Acids Res.* 1997;25(17):3389-402.

10. Grande MT, Sanchez-Laorden B, Lopez-Blau C, De Frutos CA, Boutet A, Arevalo M, Rowe RG, Weiss SJ, Lopez-Novoa JM, and Nieto MA. Snail1-induced partial epithelial-to-mesenchymal transition drives renal fibrosis in mice and can be targeted to reverse established disease. *Nat Med.* 2015;21(9):989-97.

11. Heinemeyer T, Wingender E, Reuter I, Hermjakob H, Kel AE, Kel OV, Ignatieva EV, Ananko EA, Podkolodnaya OA, Kolpakov FA, et al. Databases on transcriptional regulation: TRANSFAC, TRRD and COMPEL. *Nucleic Acids Res.* 1998;26(1):362-7.

12. Rung J, and Brazma A. Reuse of public genome-wide gene expression data. *Nat Rev Genet.* 2013;14(2):89-99.

13. Lamb J, Crawford ED, Peck D, Modell JW, Blat IC, Wrobel MJ, Lerner J, Brunet JP, Subramanian A, Ross KN, et al. The Connectivity Map: using gene-expression signatures to connect small molecules, genes, and disease. *Science.* 2006;313(5795):1929-35.

14. Hieronymus H, Lamb J, Ross KN, Peng XP, Clement C, Rodina A, Nieto M, Du J, Stegmaier K, Raj SM, et al. Gene expression signature-based chemical genomic prediction identifies a novel class of HSP90 pathway modulators. *Cancer Cell.* 2006;10(4):321-30.

15. Eden E, Lipson D, Yogev S, and Yakhini Z. Discovering motifs in ranked lists of DNA sequences. *PLoS Comput Biol.* 2007;3(3):e39.

16. Eden E, Navon R, Steinfeld I, Lipson D, and Yakhini Z. GOrilla: a tool for discovery and visualization of enriched GO terms in ranked gene lists. *BMC Bioinformatics.* 2009;10(48.

17. Szklarczyk D, Franceschini A, Wyder S, Forslund K, Heller D, Huerta-Cepas J, Simonovic M, Roth A, Santos A, Tsafou KP, et al. STRING v10: protein-protein interaction networks, integrated over the tree of life. *Nucleic Acids Res.* 2015;43(Database issue):D447-52.

18. Roider HG, Kanhere A, Manke T, and Vingron M. Predicting transcription factor affinities to DNA from a biophysical model. *Bioinformatics.* 2007;23(2):134-41.

19. Reich HN, Tritchler D, Cattran DC, Herzenberg AM, Eichinger F, Boucherot A, Henger A, Berthier CC, Nair V, Cohen CD, et al. A molecular signature of proteinuria in glomerulonephritis. *PLoS One.* 2010;5(10):e13451.

20. Schmid H, Boucherot A, Yasuda Y, Henger A, Brunner B, Eichinger F, Nitsche A, Kiss E, Bleich M, Grone HJ, et al. Modular activation of nuclear factor-kappaB transcriptional programs in human diabetic nephropathy. *Diabetes.* 2006;55(11):2993-3003.

21. Woroniecka KI, Park AS, Mohtat D, Thomas DB, Pullman JM, and Susztak K. Transcriptome analysis of human diabetic kidney disease. *Diabetes.* 2011;60(9):2354-69.

22. Flechner SM, Kurian SM, Head SR, Sharp SM, Whisenant TC, Zhang J, Chismar JD, Horvath S, Mondala T, Gilmartin T, et al. Kidney transplant rejection and tissue injury by gene profiling of biopsies and peripheral blood lymphocytes. *Am J Transplant.* 2004;4(9):1475-89.

23. Roth RB, Hevezi P, Lee J, Willhite D, Lechner SM, Foster AC, and Zlotnik A. Gene expression analyses reveal molecular relationships among 20 regions of the human CNS. *Neurogenetics.* 2006;7(2):67-80.

24. Ju W, Nair V, Smith S, Zhu L, Shedden K, Song PX, Mariani LH, Eichinger FH, Berthier CC, Randolph A, et al. Tissue transcriptome-driven identification of epidermal growth factor as a chronic kidney disease biomarker. *Sci Transl Med.* 2015;7(316):316ra193.

25. Nakagawa S, Nishihara K, Miyata H, Shinke H, Tomita E, Kajiwara M, Matsubara T, Iehara N, Igarashi Y, Yamada H, et al. Molecular Markers of Tubulointerstitial Fibrosis and Tubular Cell Damage in Patients with Chronic Kidney Disease. *PLoS One.* 2015;10(8):e0136994.

26. Chen L, Shioda T, Coser KR, Lynch MC, Yang C, and Schmidt EV. Genome-wide analysis of YY2 versus YY1 target genes. *Nucleic Acids Res.* 2010;38(12):4011-26.

27. Ko YA, Mohtat D, Suzuki M, Park AS, Izquierdo MC, Han SY, Kang HM, Si H, Hostetter T, Pullman JM, et al. Cytosine methylation changes in enhancer regions of core pro-fibrotic genes characterize kidney fibrosis development. *Genome Biol.* 2013;14(10):R108.

Full uncut gels for Figure 2C

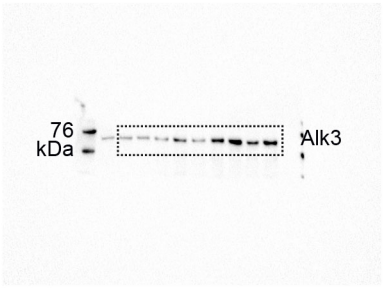

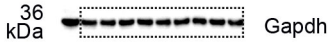

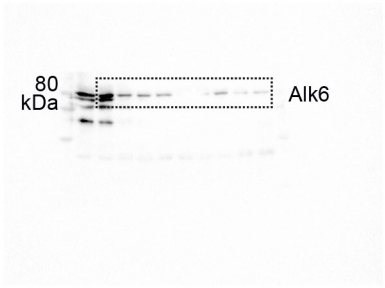

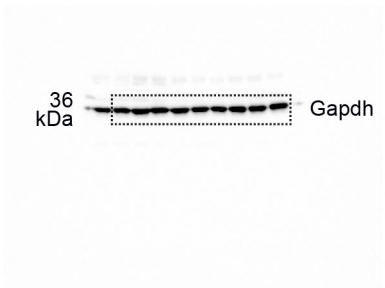

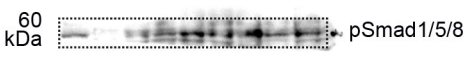

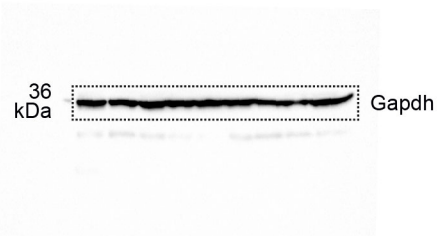

Full uncut gels for Figure 3E

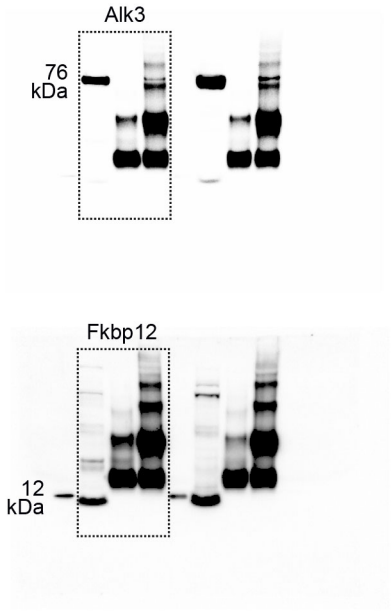

Full uncut gels for Figure 3F

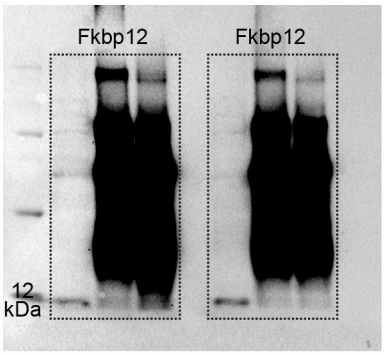

Full uncut gels for Figure 6E

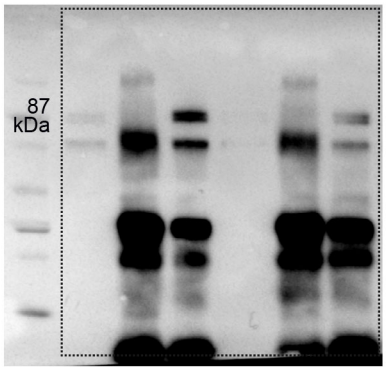

Full uncut gels for Figure 6F

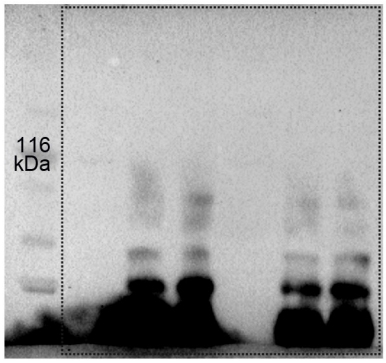

Full uncut gels for Figure 6G

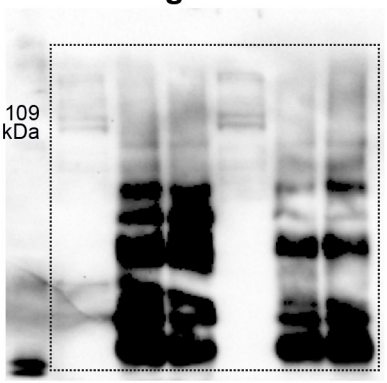

Full uncut gels for Figure 6J

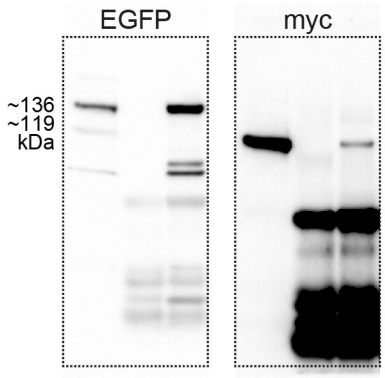

Full uncut gels for Figure 6K

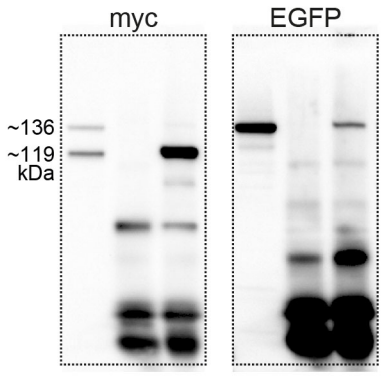

Full uncut gels for Figure 6L

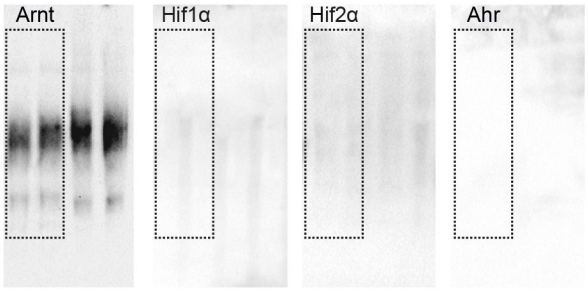

Full uncut gels for Figure 7E

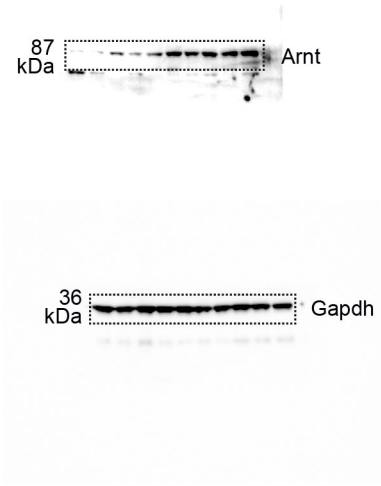

Full uncut gels for Figure 7F

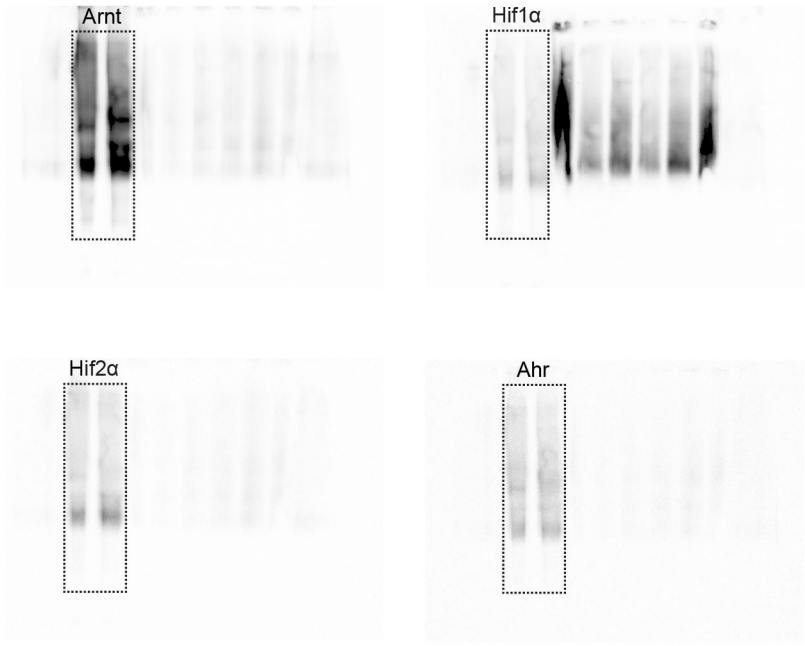

Full uncut gels for Figure 13B

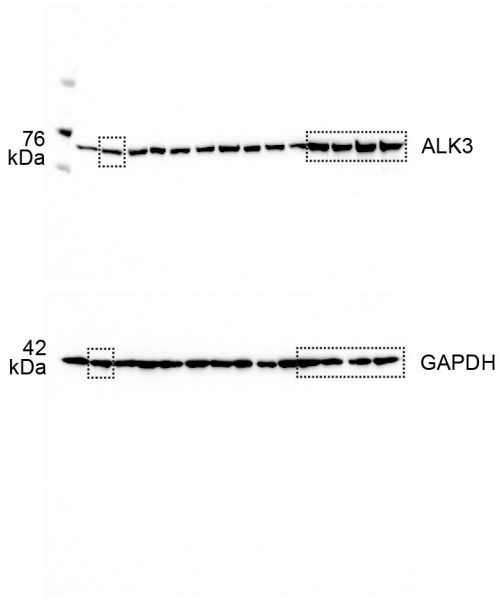

Full uncut gels for Supplementary Figure 3G

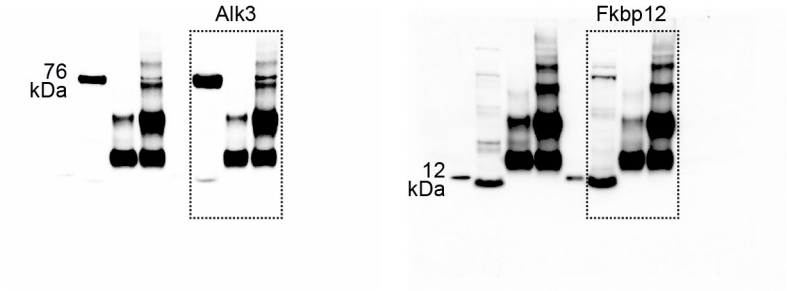

Full uncut gels for Supplementary Figure 3J

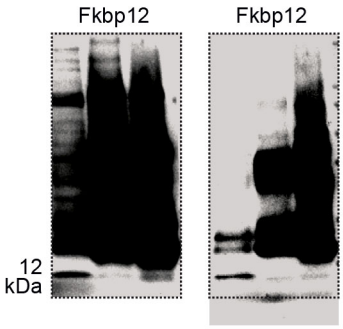

Full uncut gels for Supplementary Figure 6D

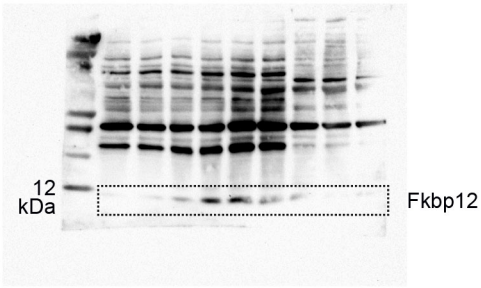

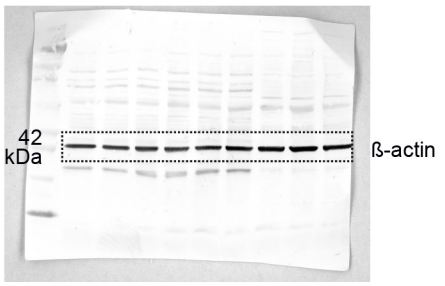

Full uncut gels for Supplementary Figure 6E

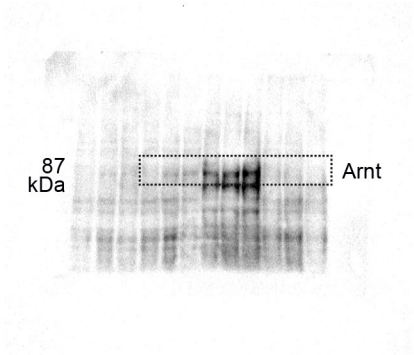

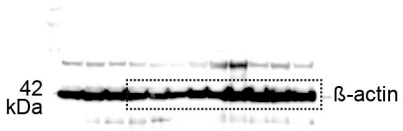

Full uncut gels for Supplementary Figure 7C